Univerzita Karlova v Praze

Matematicko-fyzikální fakulta

DIPLOMOVÁ PRÁCE

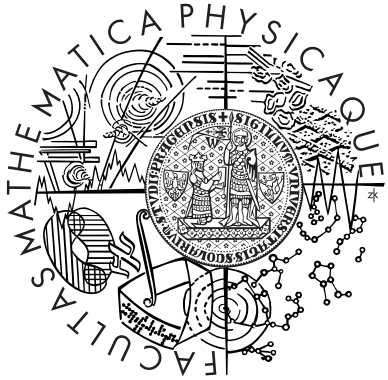

Tomáš Šikorský

Studium chirálních vlastností supramolekulárních komplexů

Vedoucí diplomové práce: doc. RNDr. Lenka Hanyková Dr.

Katedra Makromolekulární Fyziky

Studijní program: Fyzika

Studijní obor: Biofyzika a chemická fyzika

Praha 2011

Charles University in Prague

Faculty of Mathematics and Physics

DIPLOMA THESIS

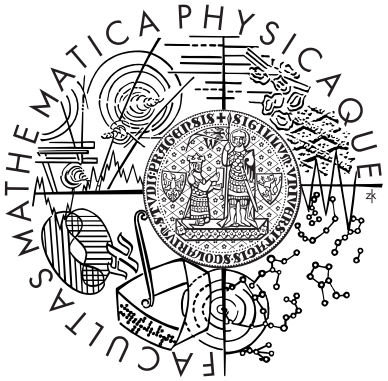

Tomas Sikorsky

Study of chiral properties of supramolecular complexes

Supervisor: doc. RNDr. Lenka Hanykova Dr.

Department of Macromolecular Physics

Study programme: Physics

Specialization: Biophysics and chemical physics

Prague 2011

I would like to thank my supervisor, Lenka Hanykova, for her support throughout this work. I would also like to thank Jaroslav Burda for his critical comments about quantum computations performed, Peter Mojzes for his support during processing of optical spectroscopy data, Jiri Bok for compiling the Fortran code that was used for fitting of titration curves and Jan Lang for his technical hints during NMR experiments.

I declare, that I have processed and written the following thesis independently, using exclusively cited sources.
I agree that this thesis shall be available in accordance with section 60 paragraph 1 of Act No. 121/2000 Coll., the Copyright Act.

In Prague; April 10, 2011 Tomas Sikorsky

Název práce: Studium chirálních vlastností supramolekulárních komplexů

Autor: Tomáš Šikorský
Katedra: Katedra makromolekulární fyziky
Vedoucí diplomové práce: doc. RNDr. Lenka Hanyková Dr.
Abstrakt: Za přítomnosti chirálního činidla, může být NMR použita jako metoda pro určení enantiomerního nadbytku u chirálních molekul. V této práci jsme se za pomoci ^{1}H-NMR spektroskopie zabývali detekci enantiomerního nadbytku Ibuprofénu (guest) použitím nechirálního porfirinógenu DiBrBzOxP (host). Detekce enantiomerního nadbytku probíhala zásluhou tvorby host-guest komplexu, kde host sloužil jako detektor. Tvorba komplexu se projevuje rozštěpením NMR signálu pyrrolových protonů DiBrBzOxP a to lineárně s enatiomerickým přebytkem Ibuprofénu. Měření taktéž ukázali, že voda se chová jako inhibitor pro tvorbu komplexu. Započtením její inhibice byla pomoci titrace určená asociační konstanta komplexu $K_a = 6.02 mol/l^{-1}$. Pro popsáni vazebného mechanizmu komplexu, byly provedeny výpočty pomoci metódy funkcionálu hustoty. Komplex byl nejprve podroben geometrické optimalizaci pomoci funkcionálu M06-L/6-31G(d,p). Pro finální struktury byli za pomoci GIAO/M06-L/6-31++G(d,p) vypočteny NMR chemické posuvy, které se následně porovnali s experimentálními hodnotami. Singulární dekompozice UV/vis a Ramanovských spekter titrovaných kyselinou trifluoroctovou odhalila existenci troch různě protonovaných forem DiBrBzOxP.
Klíčová slova: porfirinogeny, chiralita, nukleární magnetická rezonance (NMR), teorie funkcionálu hustoty (DFT), singulární rozklad (SVD)

Title: Study of chiral properties of molecular complexes
Author: Tomas Sikorsky
Department: Department of macromolecular physics
Supervisor: doc. RNDr. Lenka Hanykova Dr.
Supervisor's e-mail address: Lenka.Hanykova@mff.cuni.cz
Abstract: NMR can be used as an analytical tool for determining enantiomeric excesses of chiral molecules with use of a suitable chiral chemical shift agent. In this work we study determination of enantiomeric excesses of Ibuprofen (guest molecule) with non-chiral porphirinogen DiBrBzOxP (host molecule) using ^{1}H-NMR spectroscopy, and we report the mechanism of this phenomenon. Method is based on a formation of host-guest complex of chiral guest with achiral host signaling chiral information. This complex formation cause splitting of DiBrBzOxP's β-proton NMR resonances linearly with enantiomeric excess of the Ibuprofen. NMR studies also revealed that water acts as a inhibitor for complex formation. Considering this inhibition properties of water, association constant of DiBrBzOxP with Ibuprofen using NMR titration was determined $K_a = 6.02 mol/l^{-1}$. To understand the binding mechanism of complex, DFT computations have been performed. M06-L/6-31G(d,p) revealed two stable conformers for this complex. To verify that found structures correspond to reality, their GIAO/M06-L/6-31++G(d,p) calculated chemical shift tensors were compared to experimental values. SVD analysis of UV/vis and Raman analysis of DiBrBzOxP titrated with trifluoroacetic acid revealed existence of three different protonated forms, that might have different association constants for Ibuprofen complex.
Keywords: porphirinogens, chirality, nuclear magnetic resonance (NMR), density functional theory (DFT), singular value decomposition (SVD)

Contents

Preface

A molecule is said to be chiral if it can exist as isomers (called enantiomers) that are nonsuperimposable mirror images of each other. Response of an organism to a particular molecule depends on how the molecule fits into a binding site of a receptor molecule. Because these receptors contain chiral molecules (amino-acids, saccharides) the organisms are enantioselective. They might interact with each enantiomer differently. This is important in drug design, because about half of the drugs currently in use are chiral compounds, and many of them must be administered as pure enantiomers to produce the desired results without side effects. Maxwell's equations, which dictates chemical properties of matter, are invariant under inversion of parity. Therefore enantiomeric pairs have identical chemical properties and are indistinguishable without use of a chiral auxiliary. Chiral auxiliary methods of enantiomeric analysis include either interaction of enantiomers with circularly polarized electromagnetic waves, or their interaction with another chiral substance. Not all chiral molecules are optically active, and chirality detection with other chiral molecules has many limitations and flaws. Hence there is a great need to improve and develop new ways for determination of enantiomeric purity.

1 Nuclear magnetic resonance

1.1 Evolution of quantum state

In classical mechanics the state of a physical system is fully described by 6N parameters, where N is a number of classical point particles. Three coordinates for each particle specify its position, and other three specify its momentum in three dimensional space. The 6N parameters can be represented as a coordinates in a space, where all possible states of a given physical system are represented as a unique points[1].
The time evolution of a classical system is given by three Hamiltonian equations:

$$\frac{\partial H}{\partial q_j} = -\dot{p}_j \tag{1}$$

$$\frac{\partial H}{\partial p_j} = \dot{q}_j \tag{2}$$

$$\frac{\partial H}{\partial t} = -\frac{\partial L}{\partial t} \tag{3}$$

Hamiltonian $H(\mathbf{q}, \mathbf{p}, t)$ function is:

$$H = \sum_i q_i p_i - L \tag{4}$$

and Lagrangian $L(\mathbf{q}, \dot{\mathbf{q}}, t)$:

$$L = T(\dot{\mathbf{q}}, t) - V(\mathbf{q}, t) \tag{5}$$

T is kinetic energy $T = \frac{1}{2}\sum_i m\dot{q}_i^2$ and V is a potential energy of a system, given by its interaction with rest of the universe.
The Hamiltonian phase space canonical variables can be transformed into a new canonical variables$(q_n; p_n) \rightarrow (Q_n; P_n)$, in a way that the resulting Hamiltonian equations will be preserved, even though the Hamiltonian itself will change[2]. The new variables $(Q_n; P_n)$ generally depend on any of old variables $Q_n = Q_n(\mathbf{q}, \mathbf{p}, t)$ and $P_n = P_n(\mathbf{q}, \mathbf{p}, t)$. The transformation has the following general form:

$$H(\mathbf{q}, \mathbf{p}, t) + \frac{\partial F}{\partial t} = K(\mathbf{Q}, \mathbf{P}, t) \tag{6}$$

K is the new Hamiltonian and and F is an arbitrary differentiable function $F(q, p, Q, P, t)$, and the new variables satisfy $\{Q, P\} = 1$. Because of $Q_n = Q_n(\mathbf{q}, \mathbf{p}, t)$ and $P_n = P_n(\mathbf{q}, \mathbf{p}, t)$ only 2N of total 4N variables are independent, so F depends on 2N coordinates and time.
If we take a generating function to be $F = S(\mathbf{q}, t) = \int_{q_0,t_0}^{q,t} L(\mathbf{q}, \dot{\mathbf{q}}; t)dt$, then $\frac{\partial S(\mathbf{q},\mathbf{Q},t)}{\partial q} = \frac{\partial L(\mathbf{q},\dot{\mathbf{q}},t)}{\partial \dot{q}} = p(t)$ and also $\frac{\partial S(\mathbf{q},\mathbf{Q},t)}{\partial t} = L - \sum q_i p_i = -H$, which results in K=0. Also note that $\dot{Q} = \frac{\partial K}{\partial P}$, $\dot{P} = -\frac{\partial K}{\partial Q}$, so we now see that S is a generating function that transforms variables $(q_n; p_n) \rightarrow (Q_n; P_n)$, so that the new variables remain constant in time. Using S as a generating function for equation 6 gives Hamilton-Jacobi equation:

$$H\left(\mathbf{q}, \frac{\partial S}{\partial \mathbf{q}}, t\right) + \frac{\partial S}{\partial t} = 0 \tag{7}$$

If we take S($\mathbf{q}$,t) as a solution of particular system, $S(\mathbf{q}, t_0) = c$ defines a surface in a phase space, that describes a volume as we propagate through time. We can thus construct a gradient of a surface$\nabla S(\mathbf{q}, t_0) = m\dot{\mathbf{q}}(\mathbf{q}, t_0)$, therefore the trajectories can be obtained as perpendiculars to a surface $S(\mathbf{q}, t_0) = c$ at all times of state evolution[3] . Given the initial conditions, the state of a system is given by $S(\mathbf{q}, t)$ and its time evolution by Hamilton-Jacobi equation.

[1] The coordinates that uniquely define any possible state of the system, are also called generalized coordinates. And the space spanned by generalized coordinates is called a phase space[1]

[2] Note that the new variables, may not have the dimensions of momentum and position, but they will represent some other conjugate pair of canonical variables, such as energy and time

[3] However, this is not a case when electromagnetic fields are present, because. This problem can be solved by by introducing a non-euclidean metrics[2].

The principle of least action, which is a foundation for Hamiltonian description of classical mechanics is also a foundation for Fermat's principle, and therefore whole geometrical optics. In geometrical optics the phase velocity of a light wave in a non-homogeneous and dispersive medium, is given by[3]:

$$v = \frac{E}{\sqrt{2m(E-V)}} \tag{8}$$

Inserting this equation together with $E = \hbar\omega$ into wave equation $\left[\nabla^2 - \frac{1}{v^2}\frac{\partial^2}{\partial t^2}\right]\Psi(\mathbf{r},t) = 0$ and proposing general form of wave function $\Psi(\mathbf{r},t) = \psi(r)e^{i\omega t}$ and $\frac{\partial^2\Psi}{\partial t^2} = -\varpi^2\Psi$ results into

$$\left[\nabla^2 - \frac{2m(V-E)}{\hbar^2}\right]\psi(\mathbf{r}) = 0 \tag{9}$$

which is a time-independent non-relativistic Schrödinger equation. Multiplying this equation with $e^{i\omega t}$ to restore time dependence and realizing that $E\Psi(\mathbf{r},t) = -i\hbar\frac{\partial\Psi(\mathbf{r},t)}{\partial t}$ results in time-dependent non-relativistic Schrödinger equation:

$$\left[\nabla^2 - \frac{2m(V+i\hbar\frac{\partial}{\partial t})}{\hbar^2}\right]\Psi(\mathbf{r},t) = 0 \tag{10}$$

This equation describes the evolution of a state in quantum mechanics, where the state of the system is determined by a wave function $\Psi(\mathbf{r},t)$.

1.2 Spin

The Schrödinger equation being a non-relativistic equation is not invariant under the Lorentz transformation in space-time. This led Paul Dirac in 1928 to propose a relativistic version of Schrödinger equation[4].

$$\left[i\hbar\frac{\partial}{\partial t} + c\sum_{q=x,y,z}\alpha_q\left(i\hbar\frac{\partial}{\partial q} + eA\right) - mc^2\beta + V(\mathbf{r})\right]\bar{\mathbf{\Psi}}(\mathbf{r},\mathbf{t}) = 0 \tag{11}$$

where β and α are 4x4 matrices:

$$\alpha_x = \begin{pmatrix} 0 & 0 & 0 & 1 \\ 0 & 0 & 1 & 0 \\ 0 & 1 & 0 & 0 \\ 1 & 0 & 0 & 0 \end{pmatrix} \qquad \alpha_y = \begin{pmatrix} 0 & 0 & 0 & -i \\ 0 & 0 & i & 0 \\ 0 & -i & 0 & 0 \\ i & 0 & 0 & 0 \end{pmatrix}$$

$$\alpha_z = \begin{pmatrix} 0 & 0 & 1 & 0 \\ 0 & 0 & 0 & -1 \\ 1 & 0 & 0 & 0 \\ 0 & -1 & 0 & 0 \end{pmatrix} \qquad \beta = \begin{pmatrix} 1 & 0 & 0 & 0 \\ 0 & 1 & 0 & 0 \\ 0 & 0 & -1 & 0 \\ 0 & 0 & 0 & -1 \end{pmatrix}$$

and $\bar{\mathbf{\Psi}}(\mathbf{r},t)$ is a four-component wave-function (bispinor):

$$\bar{\mathbf{\Psi}}(\mathbf{r},t) = \begin{pmatrix} \Psi_1(\mathbf{r},t) \\ \Psi_2(\mathbf{r},t) \\ \Psi_3(\mathbf{r},t) \\ \Psi_4(\mathbf{r},t) \end{pmatrix}$$

For free particle the solution of Dirac equation leads to $E_\pm = \pm\sqrt{p^2c^2 + m_0^2c^4}$ where two energies represent particle and its twin antiparticle. Ignoring anti-particle solutions, we get two distinct wave-function solutions for particle:

[4] The combination of quantum mechanics and special relativity implies that number of particles is not conserved. Once we enter the relativistic domain we need a new formalism to treat unspecified number of particles. And there is no mechanism in non-relativistic quantum mechanics to deal with changes in particle number. Therefore any naive attempt to relativize Schrödinger equation will result in an unphysical behavior, like negative probabilities, infinite amount of negative energy states or breakdown of causality. However when these ambiguities are ignored, Dirac equation predicts existence of spin 1/2 particles.

$$\bar{\Psi}_{\mathbf{1}}(\mathbf{r},t) = \begin{pmatrix} 1 \\ 0 \\ \frac{cp_x}{m_0c^2+E} \\ \frac{c(p_y+ip_z)}{m_0c^2+E} \end{pmatrix} e^{i(\frac{\mathbf{pr}-Et}{\hbar})} \text{ and } \bar{\Psi}_{\mathbf{2}}(\mathbf{r},t) = \begin{pmatrix} 0 \\ 1 \\ \frac{c(p_y-ip_z)}{m_0c^2+E} \\ -\frac{cp_x}{m_0c^2+E} \end{pmatrix} e^{i(\frac{\mathbf{pr}-Et}{\hbar})}$$

In a non relativistic limit $v \ll c$ the third and fourth components can be neglected, and the Dirac equation can be rewritten to the following form:

$$\left[i\hbar\frac{\partial}{\partial t} - \frac{(\sigma.(-i\hbar\nabla - e\mathbf{A}))^2}{2m} - V(\mathbf{r}) \right] \bar{\Psi}(\mathbf{r},t) = 0 \tag{12}$$

where $\bar{\Psi}(\mathbf{r},t)$ is now a spinor. This form ignores relativistic effects, because it is a first order[5] approximation.
Now using identities:

$$\left[-i\hbar\frac{\partial}{\partial q_i} - eA_{i;} - i\hbar\frac{\partial}{\partial q_j} - eA_j \right] = -\epsilon_{ijk} i\hbar B_k$$

$$\sigma_i\sigma_j = \delta_{ij} + \epsilon_{ijk}\sigma_k$$

eq. 12 can be rewritten into:

$$\left[i\hbar\frac{\partial}{\partial t} - \frac{(-i\hbar\nabla - e\mathbf{A})^2}{2m} - V(\mathbf{r}) + \frac{e\hbar\sigma.\mathbf{B}}{2m} \right] \bar{\Psi}(\mathbf{r},t) = 0 \tag{13}$$

this is formally called Pauli equation, and σ is a 3 component operator, with each component acting on given component of a magnetic field. The components are:

$$\sigma_x = \begin{pmatrix} 0 & 1 \\ 1 & 0 \end{pmatrix} \qquad \sigma_y = \begin{pmatrix} 0 & -i \\ i & 0 \end{pmatrix} \qquad \sigma_z = \begin{pmatrix} 1 & 0 \\ 0 & -1 \end{pmatrix}$$

The implication of Dirac's equation is, that a relativistic description of a single particle evolution implies multiple wave functions representing particle and its twin anti-particle, and another degree of freedom for each, that we call spin. From Pauli equation we then see, that spin becomes experimentally observable as energy splitting of particle's energy, when it is exposed into magnetic field. This is basis for NMR.

1.3 Nuclear magnetic resonance spectroscopy

The general purpose of spectroscopy is characterization of a system by its spectrum. Nuclear magnetic resonance (NMR) is a spectroscopic method that measures local magnetic field strength at given nucleus. The spin particle acts as a measuring device. Its energy levels in a magnetic field are quantized, and transition among them can be induces by electromagnetic waves. For transition to occur, the frequency of electromagnetic waves that interact with spin particle must match the energy difference of spin states. Collection of frequencies that induce transition for given system defines NMR spectrum.
A traditional way to obtain a NMR spectrum, is to apply a monochromatic perturbation to the system and to measure the response. Point to point measurements allows one to trace out the spectrum. This traditional technique called "slow passage" or "continuous wave", has been used for the first 25 years of NMR spectroscopy.
Since 1970s pulse Fourier NMR spectroscopy has been replacing the old technique. It is based on a fact, that short delta function pulses can be considered as a multifrequency pulses. This pulse can simultaneously excite all resonant frequencies, and in linear systems the total response is a superposition of all individual frequency components. The reason why continuous wave NMR spectroscopy have been almost completely replaces by pulsed NMR, is not only the speed advantage. The pulsed NMR also achieves higher sensitivity and resolution.

[5] $\mathcal{O}\left(\frac{1}{c}\right)$ in cgs units

1.4 Single single particle in a magnetic field

Spin dynamics of individual spin particle, or of an ensemble of non-interacting spins can be understood by classical description where the spin of the particle is reduced to a magnetization vector. However when one wants to describe phenomenons that arise from inter-spin interaction (such as J-coupling), then it is necessary to use quantum mechanical description of a system.
If the potential term in equation (13) is independent of spin, the eigenvector solution $\bar{\mathbf{\Psi}}(\mathbf{r},t)$ can be separated into 2 parts. 1-component wave function $\Psi(\mathbf{r},t)$ on which the second and third terms in equation (13) acts and $\chi(t)$ which represents a spin state of a particle on which the first and fourth component of eq. (13) act. Because $\Psi(\mathbf{r},t)$ evolves according to magnetic field independent terms of Hamiltonian, it doesn't contribute to energy changes or state evolution when magnetic field is applied, and will be ignored. This approximation will be implicit throughout the rest of this work.
For spin 1/2 particle, the spin state can be represented as a vector in 2-dimensional complex vector space. For $\hat{S}_z = \frac{\hbar.\hat{\sigma}_z}{2}$ operator there are two orthonormal stationary states that will serve as a basis:$|\uparrow\rangle = \begin{pmatrix} 1 \\ 0 \end{pmatrix}$ and $|\downarrow\rangle = \begin{pmatrix} 0 \\ 1 \end{pmatrix}$. Defining $\hat{\mathbf{S}}^2 = \hat{S}_x^2 + \hat{S}_y^2 + \hat{S}_z^2$, we get relationships:

$$\hat{S}_q|\uparrow\rangle = \tfrac{\hbar}{2}|\uparrow\rangle \qquad \hat{S}_q|\downarrow\rangle = -\tfrac{\hbar}{2}|\downarrow\rangle \qquad \hat{\mathbf{S}}^{\mathbf{2}}|\uparrow\rangle = \tfrac{3\hbar^2}{4}|\uparrow\rangle \qquad \hat{\mathbf{S}}^{\mathbf{2}}|\downarrow\rangle = \tfrac{3\hbar^2}{4}|\downarrow\rangle$$

and these commutation relationships as well[6]:

$$\left[\hat{S}_i, \hat{S}_j\right] = \delta_{ij} + i\epsilon_{ijk}\hat{S}_k \qquad \left[\hat{\mathbf{S}}^2, \hat{S}_q\right] = 0 \text{ where } q\epsilon\{x,y,z\}$$

S being a spin of the given particle. Now if we put a particle into a static magnetic field $\mathbf{B} = \mathbf{B}(0,0,B_z)$ the equation[7] (13) will look like:

$$i\hbar\frac{\partial}{\partial t}\chi(t) = -\frac{eg\hat{S}_z.B_z}{2m}\chi(t) \tag{14}$$

Because Hamiltonian is time independent, the solution of equation (14) could be separated as:

$$\chi(t) = \exp(\frac{ieg.B_z}{4m}t)\chi(0)$$

$\chi(0) = \begin{pmatrix} \chi_1 \\ \chi_2 \end{pmatrix}$ is a spinor, given as a linear combination of two eigenstates, whose values are set by initial conditions, and each eigenstate has energy given by:

$$-\tfrac{ge\hbar B_z}{4m}\chi_1 = E_1\chi_1 \qquad \tfrac{ge\hbar B_z}{4m}\chi_2 = E_2\chi_2$$

For sake of simplicity, we can define $\omega_0 = \frac{eB_z g}{2m\hbar}$, where $\frac{g}{2}$ factor arises from quantum electrodynamics as a correction. We now see, that spin evolution in a static magnetic field is given by:

$$\chi(t) = \exp(i\varpi_{\mathbf{0}}.\hat{S}_z t)\chi(0) \tag{15}$$

Using commutation relationship $\left[\hat{S}_i, \hat{S}_j\right] = i\epsilon_{ijk}\hat{S}_k$ it can be shown that following formula applies:

$$\exp(-i\varpi.\hat{S}_k t).\hat{S}_i.\exp(i\varpi.\hat{S}_k t) = \hat{S}_i\cos(\varpi t) + \hat{S}_j\sin(\varpi t) \tag{16}$$

Therefore acting with $exp(i\varpi_{\mathbf{0}}.\hat{S}_z t)$ operator on a state $\chi(t)$ transforms the state into new state, that is rotated around z axis by angle $\varpi_{\mathbf{0}}t$. We can now simplify the analysis of $\chi(t)$ state by transforming whole equation from laboratory reference frame into reference frame that is rotating around z axis with frequency $-\varpi$. The state and operators viewed from rotating reference frame will be denoted by $\tilde{}$. Using generalized Pauli equation $i\hbar\frac{\partial}{\partial t}\chi(t) = \hat{H}(t)\chi(t)$, where $\hat{H}(t)$ denotes all operators that act on a state $\chi(t)$ from $\tilde{\chi}(t) = \exp(-i\varpi_{\mathbf{0}}.\hat{\mathbf{S}}t)\chi(t)$ we get the following

[6] For particles of different value of spin, the formalism can be build as well. Leaving the commutation relationships the same, but expanding the dimension of complex vector space to 2S+1 dimensions.

[7] corrected with $\frac{g}{2}$ factor, that arises as a consequence of quantum electrodynamics, and for purposes of NMR can be defined experimentally

transformation for $\hat{H}(t) \rightarrow \tilde{\hat{H}}(t)$: $i\hbar\frac{\partial}{\partial t}\tilde{\chi}(t) = i\hbar\left(\frac{\partial exp(-i\varpi.\hat{S}_z t)}{\partial t}.\chi(t) + \exp(-i\varpi.\hat{S}_z t).\frac{\partial\chi(t)}{\partial t}\right) = i\hbar\left(-i\varpi.\hat{S}_z.\tilde{\chi}(t) - \exp(-i\varpi.\hat{S}_z t).\frac{i}{\hbar}\hat{H}.\exp(i\varpi_{\mathbf{0}}.\hat{S}_z t)\tilde{\chi}(t)\right)$ which gives:

$$\tilde{\hat{H}}(t) = \exp(-i\varpi.\hat{S}_z t).\hat{H}.\exp(i\varpi_{\mathbf{0}}.\hat{\mathbf{S}}t) - \hbar\varpi\hat{S}_z \tag{17}$$

If we take Hamiltonian to be $\hat{H} = \hbar.\varpi_{\mathbf{0}}.\hat{S}_z + \frac{1}{2}.\frac{eg.B_{RF}}{2m}\left\{cos(\omega t)\hat{S}_x + sin(\omega t)\hat{S}_y\right\}$where first term on right hand side, refers to static magnetic field along z axis, and second term refers to oscillating magnetic field with frequency ω[8]. Transforming this Hamiltonian according to eq.(17) we get:

$$\tilde{\hat{H}} = \hbar.(\varpi_{\mathbf{0}} - \varpi).\hat{S}_z + \frac{1}{2}.\frac{eg.B_{RF}}{2m}.\exp(-i\varphi.\hat{S}_z t).\hat{S}_i.\exp(i\varphi.\hat{S}_z t) \tag{18}$$

now defining $\varpi_{nut} = \frac{1}{2}.\frac{eg.B_{RF}}{2m}$ $\varpi_{eff} = \sqrt{\varpi_{nut}^2 + (\varpi_0 - \varpi)^2}$ and $\theta = \arctan(\frac{\varpi_{nut}}{\varpi_0 - \varpi})$
It can be shown that, ignoring the relaxation, after we apply B_{RF} magnetic field, the evolution of a state will be:

$$\tilde{\chi}(t) = \exp(i\varphi.\hat{S}_z).\exp(i\theta.\hat{S}_y).\exp(i.\varpi_{eff}.\hat{S}_z.t).\exp(-i\theta.\hat{S}_y).\exp(-i\varphi.\hat{S}_z)\tilde{\chi}(0) \tag{19}$$

the relationship between state viewed from laboratory frame and from rotating frame is: $\tilde{\chi}(t) = exp(-i\varpi.\hat{S}_z t).\chi(t)$.
We now see that if pulse is applied at a Larmour frequency, its effect is to rotate a spin state by angle $\varpi_{eff}.t$ perpendicular to z-axis. If pulse is applied with frequency different than Larmour frequency, the rotation will occur about a tilted axis and will be less effective. The pulses are frequency selective. They rotate only spin states with the same Larmour frequency that they oscillate. The Larmour frequency for a given particle depends on a magnetic field at which the particle is situated.
This field can be broken into two parts:

$$\mathbf{B} = \mathbf{B}_0 + \mathbf{B}_{induced} \tag{20}$$

where magnetic field $\mathbf{B}_0$ is generated by a magnet, and $\mathbf{B}_{induced}$ is generated by other surrounding charged particles. Induced magnetic field is a consequence of externally applied magnetic field. It can be expressed as $\mathbf{B}_{induced} = \mathbf{B}_0.\delta_{\mathbf{ij}}$, where δ_{ij} is a 2nd rank tensor, which depends linearly with respect to the external magnetic field[9].
In a isotropic liquid, the shielding is equal to the isotropic shielding: $\delta = \frac{1}{3}(\delta_{xx} + \delta_{yy} + \delta_{zz})$. We can now redefine the Larmour frequency to be:

$$\omega_0 = \frac{eB_z g}{2m\hbar}(1 + \delta) \tag{21}$$

Chemical shift is defined as the difference in Larmour frequency compared to a some reference signal:

$$\frac{\omega_0 - \omega_0^{standard}}{\omega_0^{standard}} \tag{22}$$

$\omega_0^{standard}$ is a Larmour frequency of reference compound.

1.5 Ensemble of particles in a magnetic field

The particle is generally in a random, normalized superposition of states $|\uparrow\rangle$ and $|\downarrow\rangle$. The general spin state of a particle could be any linear combination of these two eigenstates: $\chi = \alpha|\uparrow\rangle + \beta|\downarrow\rangle$

[8] This part refers to linearly polarized radio frequency pulse, generated by coil, which has form $\mathbf{B_{RF}}(t) = B_x cos(\omega t) = \frac{1}{2}(B_x cos(\omega t + \varphi) + B_y sin(\omega t + \varphi)) + \frac{1}{2}(B_x cos(\omega t + \varphi) - B_y sin(\omega t + \varphi))$ of which the second part can be neglected to a good approximation.

[9] Linear behavior is as always in physics only an approximation. In this case it is a very good approximation for fields of moderate strength used in today's conventional NMR experiments.

where $\{\alpha, \beta \epsilon \mathbb{C}; \alpha\alpha^* + \beta\beta^* = 1\}$. For ensemble of N particles it is convenient to define a statistical operator as:

$$\hat{\rho} = \sum_i^N p_i \left|\chi_i\right\rangle \left\langle\chi_i\right| = \begin{pmatrix} \rho_{\alpha\alpha} & \rho_{\alpha\beta} \\ \rho_{\beta\alpha} & \rho_{\beta\beta} \end{pmatrix} \tag{23}$$

p_i are probabilities of a system to be found in the i-th state, normalized as:

$$\sum_i^N p_i = 1$$

The statistical operator has also following properties

$$\rho_{\alpha\alpha} + \rho_{\beta\beta} = 1 \text{ and } \rho_{\beta\alpha} = \rho_{\alpha\beta}^*$$

The expectation value for spin operator $\hat{S}_z$ is

$$\left\langle \hat{S}_z \right\rangle = \sum_i^N \left\langle\chi_i\right| \hat{S}_z \left|\chi_i\right\rangle = \mathrm{Tr}\left\{\hat{\rho}\hat{S}_z\right\} \tag{24}$$

And the time evolution of the statistical operator for given ensemble, is in Schrödinger representation given by Von Neumann equation as:

$$i\hbar \frac{\partial \rho(t)}{\partial t} = \left[\hat{H}, \rho\,\hat{(}t)\right] \tag{25}$$

The interpretation of statistical operator is that, $\rho_{\alpha\alpha}$ is an average contribution of each particle to expectation value of $|\uparrow\rangle$ state, and $\rho_{\beta\beta}$ is average contribution to $|\downarrow\rangle$ state. $\rho_{\alpha\beta}$ and $\rho_{\beta\alpha}$ indicate a superposition of eigenstates $|\uparrow\rangle$ and $|\downarrow\rangle$, that in NMR can be interpreted as contributions to the perpendicular spin components.
For particle in a constant magnetic filed $\mathbf{B} = \mathbf{B}(0, 0, B_z)$ and in thermal equilibrium, Boltzmann's distribution gives statistical operator:

$$\hat{\rho} = \frac{1}{\exp(\frac{eB_z g}{2mk_B T}) + \exp(-\frac{eB_z g}{2mk_B T})} \begin{pmatrix} \exp(\frac{eB_z g}{4mk_B T}) & 0 \\ 0 & \exp(-\frac{eB_z g}{4mk_B T}) \end{pmatrix} \tag{26}$$

Taking only first two terms of exponential power series $\exp(\frac{eB_z g}{4mk_B T}) \approxeq 1 + \frac{eB_z g}{4mk_B T} + ...$ the statistical operator can be approximated as:

$$\hat{\rho} \approxeq \frac{1}{2} \begin{pmatrix} 1 + \frac{eB_z g}{4mk_B T} & 0 \\ 0 & 1 - \frac{eB_z g}{4mk_B T} \end{pmatrix} = \frac{1}{2} \left(\hat{1} + \frac{e\hbar B_z g}{2mk_B t} \hat{S}_z \right) \tag{27}$$

The initial populations of energy levels are determined by equation above, therefore lower energy level contains more nuclei than the higher level.
Spin density operator, viewed from rotating frame, evolves as:

$$\tilde{\rho}_{\alpha\alpha}(t) = \tilde{\rho}_{\alpha\alpha}(0) \tag{28}$$

$$\tilde{\rho}_{\beta\beta}(t) = \tilde{\rho}_{\beta\beta}(0) \tag{29}$$

$$\tilde{\rho}_{\beta\alpha}(t) = exp\left(i\left(\varpi_0 - \varpi\right)t\right)\tilde{\rho}_{\beta\alpha}(0) \tag{30}$$

Therefore if we ignore relaxation, the evolution of an ensemble under constant magnetic field is that the population of states are constant, and coherency changes the phase, which is a quantum analog of what we would call in classical mechanics the precession. However coherences are zero in thermal equilibrium, so they need to be excited by radio frequency pulse. The evolution of each individual particle under RF pulse is depicted in eq.(19), from which the density matrix $\tilde{\rho}$ can be constructed, whose evolution will be known from equations (28-30). Therefore the difference in population $\rho_{\alpha\alpha} - \rho_{\beta\beta}$, will be transformed into coherence by RF pulse. All details of this transformation are in eq.(19).

Single particle Hamiltonian from equation 14 is not a whole story. For ensemble of particles inter-spin interactions must be considered. The effective nuclear spin Hamiltonian[10] then takes form[11]:

$$\hat{H} = \sum_i - \frac{e g_i \hat{S}_{iz}.\left(\hat{1} + \delta_{ij}\right) B_{0iz}}{2m_i} + \sum_{j<k} h.\hat{S}_j.J_{jk}.\hat{S}_k \tag{31}$$

J_{jk} is a coupling tensor, which in isotropic samples averages into scalar $\bar{J_{jk}} = \frac{1}{3}\left(J_{xx} + J_{yy} + J_{zz}\right)$. The additional term is called J-coupling. It holds for weak J-coupling, that is when $\bar{J_{jk}} \ll |\omega_j - \omega_k|$. It arises from electron mediated interactions of nuclei. The J-coupling is independent of the applied magnetic field.

J-coupling is caused by a Pauli principle. Because of that the electrons are paired in opposite spin pairs. When two nuclei are bond together by chemical bond, the states with different relative orientation of nuclear spins have different energy levels.

There are also cases when additional terms must be added. For example direct dipole-dipole coupling, which is averaged out in isotropic liquid samples, and will not be discussed here. Or Knight's shift, caused by coupling between electron and nuclear spin magnetic dipoles. Knight's shift appears only in paramagnetic samples, and it's discussion will also be omitted [8].

We now turn attention on how the expectation values of nuclear spin Hamiltonian are measured. Representing the statistical operator as a magnetization vector:

$$\mathbf{M} = N.\frac{eg}{4m}\left[2\mathrm{Re}\left\{\rho_{\beta\alpha}\right\}\hat{\mathbf{e}}_\mathbf{x} + 2\mathrm{Im}\left\{\rho_{\beta\alpha}\right\}\hat{\mathbf{e}}_\mathbf{y} + \left(\rho_{\alpha\alpha} - \rho_{\beta\beta}\right)\hat{\mathbf{e}}_\mathbf{z}\right] \tag{32}$$

The coherence gives rise to transverse magnetization, rotating with Larmour frequency around the z axis. It is the evolution of magnetization vector which is recorded in the spectrometer.

Experimentally, it was observed that even in the absence of RF field, the magnetization vector vanishes. This phenomenon is called relaxation, and in phenomenological approach of Bloch, relaxation constants T_1 and T_2 are introduced. Equation 29 is modified into:

$$\tilde{\rho}_{\beta\alpha}(t) = \exp\left[\left(i\left(\varpi_0 - \varpi\right) - \frac{1}{T_2}\right)t\right]\tilde{\rho}_{\beta\alpha}(0) \tag{33}$$

And equations 27-28 are modified as:

$$\tilde{\rho}_{\alpha\alpha}(t) = \exp\left(\frac{-t}{T_1}\right).\tilde{\rho}_{\alpha\alpha}(0) + \tilde{\rho}^{eq}_{\alpha\alpha}.\left(1 - \exp\left(\frac{-t}{T_1}\right)\right) \tag{34}$$

$$\tilde{\rho}_{\beta\beta}(t) = \exp\left(\frac{-t}{T_1}\right).\tilde{\rho}_{\beta\beta}(0) + \tilde{\rho}^{eq}_{\beta\beta}.\left(1 - \exp\left(\frac{-t}{T_1}\right)\right) \tag{35}$$

where

$$\tilde{\rho}^{eq}_{\alpha\alpha} = \tfrac{1}{2} + \tfrac{eB_z g}{8mk_BT} \qquad \tilde{\rho}^{eq}_{\beta\beta} = \tfrac{1}{2} - \tfrac{eB_z g}{8mk_BT}$$

Now we turn attention to how the time evolution of coherence, generates the resulting NMR signal. In spectrometer, the coil is aligned along any axis perpendicular to B_0 field. The voltage generated in that coil is according to Faraday's law:

$$\nabla \times (\mathbf{E}) = -\frac{\partial \mathbf{B}}{\partial t} \tag{36}$$

induced electromotive force is:

$$\varepsilon = \oint \mathbf{E}.d\mathbf{l} \tag{37}$$

Because the magnetization vector is precessing around z axis, no information will be lost if we record the electromotive force induced by only one component of $\mathbf{M}$ perpendicular to the B_0 field.

[10] The effective spin Hamiltonian unlike true spin Hamiltonian is constructed of parametric matrices fitted to experimental data. The latter is sum of differential operators determined from quantum mechanics[7].

[11] The factor of 2π arises because of J-coupling is traditionally given in hertz. I will use this standard notation, even though it introduces a useless complications of some equations.

Assuming that the observable quantity, also called free induction decay (FID) is proportional to electromotive force, combining equations 32, 36 and 37 gives:

$$s_{FID}(t) \propto \frac{\partial \mathrm{Re}\left\{\rho_{\beta\alpha}\left(t\right)\right\}}{\partial t} \tag{38}$$

referring to equation 31 we obtain:

$$s_{FID}(t) \propto \left[i\left(\varpi_0 - \varpi\right) - \frac{1}{T_2}\right] \mathrm{Im}\left\{\rho_{\beta\alpha}\left(t\right)\right\} \tag{39}$$

Where $\frac{1}{T_2} \ll (\varpi_0 - \varpi)$, and $\frac{1}{T_2}$ is therefore omitted.
After FID is amplified, it is mixed with receiver reference signal, and with $\frac{\pi}{2}$ shifted receiver reference signal

$$s_{FID}(t).s_{RRS}(t) \propto \left[i\left(\varpi_0 - \varpi\right)\right] \mathrm{Im}\left\{\rho_{\beta\alpha}\left(t\right)\right\}.\cos\left(\varpi_{ref}.t + \varphi_{ref}\right) \tag{40}$$

$$s_{FID}(t).s_{RRS}^{shifted}(t) \propto \left[i\left(\varpi_0 - \varpi\right)\right] \mathrm{Im}\left\{\rho_{\beta\alpha}\left(t\right)\right\}.\cos\left(\varpi_{ref}.t + \varphi_{ref} + \frac{\pi}{2}\right) \tag{41}$$

Equations 38 and 39, under transformation into rotating frame, and removing $(\varpi_0 - \varpi) + \varpi_{ref}$ components of oscillation by filter, can be simplified into following form:

$$s^{normal}(t) \propto i.\mathrm{Im}\left\{\tilde{\rho}_{\beta\alpha}\left(t\right)\right\}\sin(\varphi_{ref}) \tag{42}$$

$$s^{shifted}(t) \propto \mathrm{Re}\left\{\tilde{\rho}_{\beta\alpha}\left(t\right)\right\}\cos(\varphi_{ref}) \tag{43}$$

Now summing above two contributions, we finally receive:

$$s(t) \propto i\tilde{\rho}_{\beta\alpha}\left(t\right)\exp(i.\varphi_{ref}) \tag{44}$$

We now see, that voltage generated by NMR coil is proportional to the coherency of spin ensemble.
If we now substitute eq.(31) into equation(42) we get:

$$s(t) \propto exp\left[\left(i\left(\varpi_0 - \varpi\right) - \frac{1}{T_2}\right)t\right] \tag{45}$$

To determine frequencies present in a spectrum, mathematical technique which transforms function (43), into equivalent function of frequency variable, is used. The technique is called Fourier transformation and is defined as:

$$S\left(\Omega\right) = \int_{\mathbb{R}^+} s(t)\exp\left(-i\Omega t\right)dt \tag{46}$$

Where $\Omega = \varpi_0 - \varpi$. The effect of this transformation, is to visualize the frequency components of a $s(t)$.

1.6 J-coupling

NMR spectrum contains more information than just the chemical shift. As already pointed out in equation (31) J-coupling is another phenomenon that alters the appearance of NMR spectrum. J-coupling is electron mediated dipole-dipole interaction of nuclei. Because it is mediated by electrons, it occurs only between nuclei among the same molecule, and is not averaged out in isotropic liquids. The effect of J-coupling is to split the NMR signals into a multiplet.
The mechanism that is responsible for the J-coupling can be described as follows. Every electron interacts with its own nucleus's dipolar magnetic field. The interaction energy is proportional to:

$$E \propto g_e g_n \hat{\mathcal{S}}_e.\hat{\mathcal{S}}_n \tag{47}$$

There are two important facts that should be deduced from equation above. First is that antiparallel orientation of spins gives lower energy state. Second is that interaction is, unlike chemical shift, independent of magnetic field.

This short range interaction between electron and it's nucleus is mediated through bonding electrons and induce inter-nuclei interactions. This happens because of Pauli exclusion principle. Two electrons that reside in the same bonding orbital must have anti-parallel orientation of spins. But J-coupling is observed even between nuclei that are connected through more bonds. This occurs if atoms that mediate the connection are found in a triplet state. The orientation of the e-th nucleus's spin interacts with spin of n-th nuclei.

Now let's assign anti-parallel orientation of electron and it's nucleus as $|\alpha\rangle$ and parallel orientation as $|\beta\rangle$. In case of two interacting nuclei we will have four orthogonal energy states: $|\alpha\alpha\rangle$, $|\alpha\beta\rangle$, $|\beta\alpha\rangle$, $|\beta\beta\rangle$. These states are eigenstates of non interacting Hamiltonian.

J coupling is observed during NMR transitions. For example when$|\alpha\rangle \rightarrow |\beta\rangle$ occurs, it would normally result in signal corresponding to shifted Larmour frequency of a given nucleus. But now because of J-interaction the resonance frequency of e-th nucleus coupled to n-th nucleus the frequency is perturbed.

The four states outlined above lead to four transitions observed in NMR experiment[12]: $|\alpha\alpha\rangle \rightarrow |\alpha\beta\rangle, |\alpha\alpha\rangle \rightarrow |\beta\alpha\rangle, |\alpha\beta\rangle \rightarrow |\beta\beta\rangle, |\beta\alpha\rangle \rightarrow |\beta\beta\rangle$, the first letter refers to e-th particle, and second refers to the n-th particle.

Now we need to determine the energy levels of these transitions. So the Hamiltonian matrix for these states must be constructed. We will use Hamiltonian equation 31, and introduce following notation: $\Delta = \omega_I - \omega_J$ and $\delta = \frac{1}{2}(\omega_I + \omega_J)$. Also note that J is in hertz, in contrast to all other frequencies that are used in this work.

$$\langle\alpha\alpha|\hat{H}|\alpha\alpha\rangle = \hbar\left(-\delta + 2\pi\frac{J}{4}\right)$$

$$\langle\alpha\beta|\hat{H}|\alpha\beta\rangle = \hbar\left(-\frac{\Delta}{2} - 2\pi\frac{J}{4}\right)$$

$$\langle\beta\alpha|\hat{H}|\beta\alpha\rangle = \hbar\left(\frac{\Delta}{2} - 2\pi\frac{J}{4}\right)$$

$$\langle\beta\beta|\hat{H}|\beta\beta\rangle = \hbar\left(\delta + 2\pi\frac{J}{4}\right)$$

Anti-parallel spin arrangements are lowered in energy by $\frac{J}{4}$ and parallel are raised by same amount.

All non-diagonal parts are zero except $\langle\alpha\beta|\hat{H}|\beta\alpha\rangle$ and $\langle\beta\alpha|\hat{H}|\alpha\beta\rangle$. To solve for them, we need to employ:

$$\hat{S}_I\hat{S}_J = \frac{1}{2}\left(\hat{S}_{I^+}.\hat{S}_{J^-} + \hat{S}_{I^-}.\hat{S}_{J^+}\right) + S_{I_z}S_{J_z}$$

where the so-called ladder operators: $\hat{S}_{I(J)^\pm} = \hat{S}_{I(J)^x} \pm i\hat{S}_{I(J)^y}$ have following effects: $\hat{S}_{I(J)^+}|\alpha(\alpha)\rangle = |\beta(\beta)\rangle$ and $\hat{S}_{I(J)^-}|\alpha(\alpha)\rangle = 0$ $\hat{S}_{I(J)^+}|\beta(\beta)\rangle = 0$ and $\hat{S}_{I(J)^-}|\beta(\beta)\rangle = |\beta(\beta)\rangle$.

Therefore $\langle\alpha\beta|\hat{H}|\beta\alpha\rangle = \langle\alpha\beta|\left(-\hbar\omega_I\hat{S}_{I_z} + \hbar\omega_J\hat{S}_{J_z}\right) - h.J_{IJ}\left(\frac{1}{2}\left(\hat{S}_{I^+}.\hat{S}_{J^-} + \hat{S}_{I^-}.\hat{S}_{J^+}\right) + \hat{S}_{I_z}\hat{S}_{J_z}\right)|\beta\alpha\rangle$, but because the states are orthogonal, and are also eigenstates of angular momentum operator, the equations simplifies into:

$$\langle\alpha\beta|\hat{H}|\beta\alpha\rangle = \langle\alpha\beta| - h.J_{IJ}\left(\hat{S}_{I^+}.\hat{S}_{J^-} + \hat{S}_{I^-}.\hat{S}_{J^+}\right)|\beta\alpha\rangle = h.\frac{J}{2}$$

Therefore:

$$\langle\alpha\beta|\hat{H}|\beta\alpha\rangle = h.\frac{J}{2}$$

$$\langle\beta\alpha|\hat{H}|\alpha\beta\rangle = h.\frac{J}{2}$$

Hamiltonian (equation 31) in matrix representation with basis $\{|\alpha\alpha\rangle, |\alpha\beta\rangle, |\beta\alpha\rangle, |\beta\beta\rangle\}$ is:

$$\begin{pmatrix} \hbar\left(-\delta + 2\pi\frac{J}{4}\right) - E & 0 & 0 & 0 \\ 0 & \hbar\left(-\frac{\Delta}{2} + 2\pi\frac{J}{4}\right) - E & h.\frac{J}{2} & 0 \\ 0 & h.\frac{J}{2} & \hbar\left(\frac{\Delta}{2} + 2\pi\frac{J}{4}\right) - E & 0 \\ 0 & 0 & 0 & \hbar\left(\delta + 2\pi\frac{J}{4}\right) - E \end{pmatrix} \begin{pmatrix} c_1 \\ c_2 \\ c_3 \\ c_4 \end{pmatrix} = 0$$

[12]Because for a observable transition of nucleus e, the magnetic moment, and therefore also a state of nucleus n must be unchanged.

Energies of eigenstates $\langle\alpha\alpha|\,\hat{H}\,|\alpha\alpha\rangle$ and $\langle\beta\beta|\,\hat{H}\,|\beta\beta\rangle$ are already known, because they have no off-diagonal elements. The task is now do determine the other two states. This can be achieved by solving the eigenvalue problem:

$$\begin{pmatrix} \hbar\left(-\frac{\Delta}{2}+2\pi\frac{J}{4}\right)-E & h.\frac{J}{2} \\ h.\frac{J}{2} & \hbar\left(\frac{\Delta}{2}+2\pi\frac{J}{4}\right)-E \end{pmatrix}\begin{pmatrix} c_2 \\ c_3 \end{pmatrix}=0 \tag{48}$$

energies of two eigenstates can be found by solving determinant:

$$\begin{vmatrix} \hbar\left(-\frac{\Delta}{2}+2\pi\frac{J}{4}\right)-E & h.\frac{J}{2} \\ h.\frac{J}{2} & \hbar\left(\frac{\Delta}{2}+2\pi\frac{J}{4}\right)-E \end{vmatrix}=0 \tag{49}$$

which has solution $E_{\pm}=-h\frac{J}{4}\pm\frac{1}{2}\sqrt{\frac{h^2J^2}{4}-4\left(\frac{h^2J^2}{16}-\frac{h^2J^2}{4}-\frac{\hbar^2\delta^2}{4}\right)}=-h\frac{J}{4}\pm\frac{1}{2}\sqrt{h^2J^2+\hbar^2\Delta^2}$ and eigenvalues for E_+ are $c_2=\sin(\theta)$ and $c_3=\cos(\theta)$ and for E_- $c_2=\cos(\theta)$ and $c_3=-\sin(\theta)$, where $\tan(2\theta)=\frac{\pi J}{\delta}$.
Energies of four transitions are:

$$E_{|\alpha\alpha\rangle\rightarrow\cos(\theta)|\alpha\beta\rangle-\sin(\theta)|\beta\alpha\rangle}=\hbar\delta-h\frac{J}{2}-\frac{1}{2}\sqrt{h^2J^2+\hbar^2\Delta^2}=E_1$$

$$E_{|\alpha\alpha\rangle\rightarrow\sin(\theta)|\alpha\beta\rangle+\cos(\theta)|\beta\alpha\rangle}=\hbar\delta-h\frac{J}{2}+\frac{1}{2}\sqrt{h^2J^2+\hbar^2\Delta^2}=E_2$$

$$E_{\cos(\theta)|\alpha\beta\rangle-\sin(\theta)|\beta\alpha\rangle\rightarrow|\beta\beta\rangle}=\hbar\delta+h\frac{J}{2}+\frac{1}{2}\sqrt{h^2J^2+\hbar^2\Delta^2}=E_3$$

$$E_{\sin(\theta)|\alpha\beta\rangle+\cos(\theta)|\beta\alpha\rangle\rightarrow|\beta\beta\rangle}=\hbar\delta+h\frac{J}{2}-\frac{1}{2}\sqrt{h^2J^2+\hbar^2\Delta^2}=E_4$$

Frequencies of spectral lines are given by this four transition energies. The average chemical shift δ, J-coupling constant J and difference in shielding between J-coupled protons Δ can be found by these algebraic operations:

$$\delta=\frac{E_1+E_2+E_3+E_4}{4\hbar}$$

$$\Delta=\frac{\sqrt{(E_4-E_2).(E_1-E_3)}}{\hbar}$$

$$J=\frac{E_3-E_2}{h}=\frac{E_4-E_1}{h}$$

Their corresponding intensities depend on transition probabilities and populations of initial states. Because the transition energies are much lower than k_BT, we can assume that all levels are equally populated. Therefore intensities are proportional only to transition probabilities given by:

$$I_{|\alpha\alpha\rangle\rightarrow\cos(\theta)|\alpha\beta\rangle-\sin(\theta)|\beta\alpha\rangle}\propto\langle\alpha\alpha|\,\hat{S}_{J_x}\,|\cos(\theta)\,\alpha\beta\rangle-\langle\alpha\alpha|\,\hat{S}_{I_x}\,|\sin(\theta)\,\beta\alpha\rangle=1-\frac{J}{\sqrt{J^2+\frac{\Delta^2}{2\pi}}}$$

$$I_{|\alpha\alpha\rangle\rightarrow\sin(\theta)|\alpha\beta\rangle+\cos(\theta)|\beta\alpha\rangle}\propto\langle\alpha\alpha|\,\hat{S}_{J_x}\,|\sin(\theta)\,\alpha\beta\rangle+\langle\alpha\alpha|\,\hat{S}_{I_x}\,|\cos(\theta)\,\beta\alpha\rangle=1+\frac{J}{\sqrt{J^2+\frac{\Delta^2}{2\pi}}}$$

$$I_{\cos(\theta)|\alpha\beta\rangle-\sin(\theta)|\beta\alpha\rangle\rightarrow|\beta\beta\rangle}\propto\langle\beta\beta|\,\hat{S}_{J_x}\,|\cos(\theta)\,\alpha\beta\rangle-\langle\alpha\alpha|\,\hat{S}_{I_x}\,|\sin(\theta)\,\beta\alpha\rangle=1-\frac{J}{\sqrt{J^2+\frac{\Delta^2}{2\pi}}}$$

$$I_{\sin(\theta)|\alpha\beta\rangle+\cos(\theta)|\beta\alpha\rangle\rightarrow|\beta\beta\rangle}\propto\langle\beta\beta|\,\hat{S}_{J_x}\,|\sin(\theta)\,\alpha\beta\rangle+\langle\alpha\alpha|\,\hat{S}_{I_x}\,|\cos(\theta)\,\beta\alpha\rangle=1+\frac{J}{\sqrt{J^2+\frac{\Delta^2}{2\pi}}}$$

It is now obvious that for $\Delta\neq0$ a spectrum looks like a pair of roofing doublets.
Equations discussed above were taken from [6], [7], [8].

2 Quantum chemistry

2.1 Density Functional Theory

"We can judge of the perfection to which a science has come by the facility, more or less great, with which it may be approached by calculation." [9]
Adolphe Quetelet

At a molecular level[13], Schrödinger equation (10) describes most of the fundamental properties of matter[14]. The problem is, that solutions of Schrödinger equation is a wave-function of 3N spacial coordinates [15], which means that solving it for molecules is computationally very demanding. But for purposes of finding accurate description of a quantum system an alternative approach can be used. It is a density functional theory (DFT), that do not operates with wave-function, but uses a ground state electron density function instead [10]:

$$\rho(\mathbf{r}) = \sum_{\mathbf{i}}^{\mathbf{N}} \int ... \int |\mathbf{\Psi}\left(\mathbf{r_1}, \mathbf{r_2}, ...\mathbf{r_N}\right)|^{\mathbf{2}} \prod_{\mathrm{j}\neq\mathrm{i}}^{\mathrm{N}} \mathrm{d}\mathbf{r_j} \tag{50}$$

But because the wave-function is anti-symmetric under particle interchange, this equation can be simplified into:

$$\rho(\mathbf{r}) = \mathbf{N} \int ... \int |\mathbf{\Psi}\left(\mathbf{r}, \mathbf{r_2}, ...\mathbf{r_N}\right)|^{\mathbf{2}} \prod_{\mathrm{i}=2}^{\mathrm{N}} \mathrm{d}\mathbf{r_i} \tag{51}$$

Also the number of electrons is

$$N = \int \rho(\mathbf{r}) d\mathbf{r} \tag{52}$$

The Hohenberg–Kohn theorem says that for a system of interacting elementary particles, a bijective projection from a ground state electronic density function to a Hamiltonian of a given system exists. Because Hamiltonian determines the wave-function and energy of a given system, a functional of ground state electron density that gives us energy of a system also exists[11].
We now see, that the quantity of physical interest, is a probability of finding an electron within infinitesimal volume element (dx,dy,dz). But how energy of a system can be extracted from this electron density function?
The idea is based on Schrödinger equation (10). Hamiltonian for N-electron system could be written in a following form:

$$\mathbf{\hat{H}} = \mathbf{\hat{T}} + \mathbf{\hat{V}} + \mathbf{\hat{U}} \tag{53}$$

$\hat{T}$ is part describing kinetic energy of electrons $\hat{T} = -\sum_{i}^{N} \frac{\hbar^2}{2m_e} \nabla_i^2$, $\hat{U}$ describes electrostatic electron-electron repulsion $\hat{U} = \frac{1}{2} \sum_{i \neq j}^{N} \frac{e'^2}{|\mathbf{r}_i - \mathbf{r}_j|}$ and $\hat{V}$ is a term describing electrostatic interaction of electrons with protons$\hat{V} = -\sum_{i}^{N} \sum_{\alpha} \frac{e'^2 Z_\alpha}{|\mathbf{r}_i - \mathbf{r}_\alpha|}$ where Z_α is the charge of $\alpha - th$ nucleus and $e'^2 = \frac{e^2}{4\pi\epsilon_0}$.
Because the $\mathbf{\hat{V}}$ does not contain any derivatives, we may take the wave-function and its conjugate under a conjugate square:

$$\left\langle \Psi\left(\mathbf{r_1}, \mathbf{r_2}, ...\mathbf{r_N}\right) \right| \hat{V} \left| \Psi\left(\mathbf{r_1}, \mathbf{r_2}, ...\mathbf{r_N}\right) \right\rangle = -\sum_{i}^{N} \sum_{\alpha} \int \frac{e'^2 Z_\alpha}{|\mathbf{r}_i - \mathbf{r}_\alpha|} \left| \Psi\left(\mathbf{r_1}, \mathbf{r_2}, ...\mathbf{r_N}\right) \right|^2 \prod_{\mathrm{i}=1}^{\mathrm{N}} \mathrm{d}\mathbf{r_i} \tag{54}$$

[13] By molecular level, I mean an approximation, where electrons, protons and neutrons are considered as elementary particles.

[14] One very important property of particles, their spin, is absent in Schrödinger equation. This leads to violation of Pauli's exclusion principle. Expressing the wave-function as a Slater determinant introduces the required anti-symmetry (the wave-function should be anti-symmetric under particle exchange) and consequently also satisfies the Pauli's exclusion principle.

[15] where N is a number of elementary particles in a system

in each i-th term, we can separate r_i variable from others:

$$\langle \Psi(\mathbf{r_1},\mathbf{r_2},...\mathbf{r_N})|\,\hat{V}\,|\Psi(\mathbf{r_1},\mathbf{r_2},...\mathbf{r_N})\rangle = -\sum_i^N \sum_\alpha \int \frac{e'^2 Z_\alpha}{|\mathbf{r}_i - \mathbf{r}_\alpha|} d\mathbf{r_i} \int ... \int |\Psi(\mathbf{r}_1,\mathbf{r_2},...\mathbf{r_N})|^2 \prod_{\mathrm{j}\neq\mathrm{i}}^{\mathrm{N}} \mathrm{d}\mathbf{r_j} \tag{55}$$

On the right side, we recognize, the electron density function. Summing the equation under i-th index, we get:

$$\langle \Psi(\mathbf{r_1},\mathbf{r_2},...\mathbf{r_N})|\,\hat{V}\,|\Psi(\mathbf{r_1},\mathbf{r_2},...\mathbf{r_N})\rangle = -\sum_\alpha \int \rho(\mathbf{r}) \frac{e'^2 Z_\alpha}{|\mathbf{r} - \mathbf{r}_\alpha|} d\mathbf{r} = -\int \rho(\mathbf{r})\, v(\mathbf{r})\, d\mathbf{r} \tag{56}$$

$v(\mathbf{r}) = \sum_\alpha \frac{e'^2 Z_\alpha}{|\mathbf{r}-\mathbf{r}_\alpha|}$

However, the expectation value of $\hat{U}$ operator, can not be written as a functional of single particle density. Because of this, we are forced to make an approximation:

$$\langle \Psi(\mathbf{r_1},\mathbf{r_2},...\mathbf{r_N})|\,\hat{U}\,|\Psi(\mathbf{r_1},\mathbf{r_2},...\mathbf{r_N})\rangle = \frac{1}{2}\int\int \frac{\rho(\mathbf{r}')\,\rho(\mathbf{r}')}{|\mathbf{r}-\mathbf{r}'|} d\mathbf{r} d\mathbf{r}' + E_{ee}[\rho(\mathbf{r})] \tag{57}$$

the first part, is the energy of electrostatic electron-electron interaction as if all electrons were completely uncorrelated, and the correlation term $E_{ee}[\rho(\mathbf{r})]$ is unknown functional of electron density.
Value of $\hat{T}$ is even bigger problem. Since the operator includes second derivatives, there is no way how can this be rewritten into functional of electron density function. We therefore express this term in terms of Kohn-Sham orbital functions as sum of a non-interacting system of electrons and unknown term $E_T[\rho(\mathbf{r})]$:

$$\langle \Psi(\mathbf{r_1},\mathbf{r_2},...\mathbf{r_N})|\,\hat{T}\,|\Psi(\mathbf{r_1},\mathbf{r_2},...\mathbf{r_N})\rangle = -\frac{\hbar^2}{2m_e}\sum_i^N \left\langle \Psi_i^{KS}(\mathbf{r})\right| \nabla_i^2 \left|\Psi_i^{KS}(\mathbf{r})\right\rangle + E_T[\rho(\mathbf{r})] \tag{58}$$

Kohn-Sham orbital functions are eigenfunctions of a fictitious system of non-interacting electrons and $E_T[\rho(\mathbf{r})]$ is kinetic energy difference between non-interacting system and real one. Kohn-Sham orbital functions can be obtained from:

$$\left[-\frac{\hbar^2}{2m_e}\nabla_i^2 + v_s(\mathbf{r}) - \varepsilon_i\right]\Psi_i^{KS}(\mathbf{r}) = 0 \tag{59}$$

ε_i is the eigenvalue, and $v_s(\mathbf{r})$ is a potential chosen in a way, as to make a probability density $\rho_s(\mathbf{r}) = \sum_i^N \left|\Psi_i^{KS}(\mathbf{r})\right|^2$ equals to $\rho(\mathbf{r})$.
Defining the exchange correlation functional by $E_{xc}[\rho(\mathbf{r})] = E_T[\rho(\mathbf{r})] + E_{ee}[\rho(\mathbf{r})]$ we have:

$$E[\rho(\mathbf{r})] = -\frac{\hbar^2}{2m_e}\sum_i^N \left\langle \Psi_i^{KS}(\mathbf{r})\right| \nabla_i^2 \left|\Psi_i^{KS}(\mathbf{r})\right\rangle + \frac{1}{2}\int\int \frac{\rho(\mathbf{r}')\,\rho(r')}{|\mathbf{r}-\mathbf{r}'|} d\mathbf{r} d\mathbf{r}' - \int \rho(\mathbf{r})\, v(\mathbf{r})\, d\mathbf{r} + E_{xc}[\rho(\mathbf{r})] \tag{60}$$

The total energy also includes the electrostatic repulsion between the protons, whose positions are parameters in a DFT problem, therefore are unimportant in procedure of finding the electron density function:

$$E_{tot} = E[\rho(\mathbf{r})] + \sum_{\alpha\neq\beta} \frac{e'^2 Z_\alpha Z_\beta}{|r_\alpha - r_\beta|} \tag{61}$$

Another theorem, proven by Hohenberg and Kohn states, that any trial positive electron density function $\rho_{tr}(\mathbf{r})$, satisfying equation (52) plugged into equation (60) satisfies following inequality [12]:

$$E[\rho(\mathbf{r})] \leqq E[\rho_{tr}(\mathbf{r})] \tag{62}$$

In order to vary density function to find lowest possible energy, there are two things that need to be determined:

1. a functional $E_{xc}[\rho(\mathbf{r})]$
2. a potential $v_s(\mathbf{r})$

Eventually we can vary Kohn-Sham orbitals[16], which determine density function, when proper form of potential $v_s(\mathbf{r}_i)$ is chosen. It can be shown that the proper form is [13]:

$$v_s(\mathbf{r}) = -\sum_\alpha \frac{e'^2 Z_\alpha^2}{|r - r_\alpha|} + \int \frac{e'^2 \rho(\mathbf{r}')}{|r - r'|} d\mathbf{r}' + \frac{\delta E_{xc}[\rho(\mathbf{r})]}{\delta \rho(\mathbf{r})} \tag{63}$$

Problem now is, that to solve Kohn-Sham equation we need to know electron density function. But the electron density function could be calculated from Kohn-Sham orbital functions which are given by Kohn-Sham equation. To break this circle, the problem can be solved by an iterative process.

This process is based on idea, that equation (63) is true only for ground state density function. We can guess the density function, insert it into eq. (63), and from Kohn-Sham orbitals we can construct another density function. Comparing constructed function, with our initial guess we can analyze how close to ground state our guess was. This is a crucial fact, that allows us to design iterative process, that finds ground state density function.

So equations (63) and (61) could in principle be used to find an exact density function, as would be found by solving Schrödinger equation (10). The problem is that we do not know the precise form of the exchange–correlation functional[17]. Therefore we must rely on empirical forms of this functional. This is what makes DFT an empirical theory, in contrast with Hartree-Fock and post Hartree-Fock methods. It has been said that [14] "while solutions to the HF equations may be viewed as exact solutions to an approximate description, the KS equations are approximations to an exact description."

2.2 Calculation of NMR parameters

Experimental spectra of simple molecules, can be interpreted empirically, but in more difficult cases, the theoretical computations can be very helpful. And not only they are helpful, but they also provide a direct link between observed NMR spectra and electronic structure of a measured system.

The computations are done using spin Hamiltonian. As noted earlier in this work, while effective spin Hamiltonian is experimentally parametrized, the true spin Hamiltonian arises from quantum mechanics. The aim of quantum mechanical computations is to create a link between them[15]. Magnetic shielding tensor is defined as:

$$\delta_{ij} = -\frac{B_i^{induced}}{B_j} \tag{64}$$

Because a magnetic field calculated by the Biot–Savart law will always satisfy Gauss's law for magnetism and Ampere's law, $B^{induced}$ is given as:

$$\mathbf{B}_{induced}(\mathbf{r}) = \frac{\mu_0}{4\pi} \int \frac{\mathbf{j}(\mathbf{r}' - \mathbf{r}) \times (\mathbf{r}' - \mathbf{r})}{|\mathbf{r}' - \mathbf{r}|^3} d\mathbf{r}' \tag{65}$$

To calculate the $\mathbf{j}(\mathbf{r}')$ we have to perform a calculation in presence of the external magnetic field $\mathbf{B^0}$. This can be done, by augmenting the Hamiltonian by magnetic potential, which within a Coulomb gauge looks:

$$\mathbf{A}(\mathbf{r}) = \frac{1}{2}\mathbf{B}(\mathbf{r}) \times (\mathbf{r} - \mathbf{R}) \tag{66}$$

$\mathbf{R}$ is a gauge origin and can be chosen arbitrarily.

Therefore Hamiltonian of equation (53) will be transformed into following augmented form:

$$\hat{H} = \hat{H}_0 - \frac{ie\hbar}{4m}[(\mathbf{r} - \mathbf{R}) \times \nabla]\mathbf{B_0} + \frac{e^2}{16m}[\mathbf{B} \times (\mathbf{r} - \mathbf{R})]^2 \tag{67}$$

[16] Their orthonormality must be conserved

[17] This statement applies to year 2010.

The current density for closed shell systems is given by the electronic wave-function:[18]

$$\mathbf{j}(\mathbf{r}) = \frac{i\hbar}{m}\sum_i \nabla\Psi_i^*(\mathbf{r})\,\Psi_i(\mathbf{r}) - \nabla\Psi_i(\mathbf{r})\,\Psi_i^*(\mathbf{r}) - 2\mathbf{A}\sum_i \Psi_i^*(\mathbf{r})\,\Psi_i(\mathbf{r}) \tag{68}$$

Because in NMR the induced current density is linear in the strength of the field, we are justified to perform calculations in the limit $\mathbf{B} \to 0$, and also only terms in first order of $\mathbf{B}$ are needed. Hamiltonian and its orbitals are thus expanded into following series:

$$\hat{H} = \hat{H}^{(0)} + \frac{ie\hbar}{4m}\left[(\mathbf{r}-\mathbf{R})\times\nabla\right]\mathbf{B_0} + \mathcal{O}\left(B^2\right) \tag{69}$$

$$\Psi = \Psi^{(0)} + i\Psi^{(1)} + \mathcal{O}\left(B^2\right) \tag{70}$$

So the current density can be thus expanded in a similar way:

$$j = j^0 + ij^1 + \mathcal{O}\left(B^2\right) \tag{71}$$

Where the 0-th terms are terms if magnetic field vanishes, and 1-th terms are linear responses. For current density, j^0 vanishes in the absence of a magnetic field and its linear response is [16]:

$$\mathbf{j^1}(\mathbf{r}) = \frac{\hbar}{m}\sum_i \nabla\Psi_i^{(1)}(\mathbf{r})\,\Psi_i^{(0)}(\mathbf{r}) - \nabla\Psi_i^{(0)}(\mathbf{r})\,\Psi_i^{(1)}(\mathbf{r}) - 2\mathbf{A}\sum_i \Psi_i^{(0)}(\mathbf{r})\,\Psi_i^{(0)}(\mathbf{r}) \tag{72}$$

When the first order current density is considered in Biot-Savard's law, one obtains the following equation for shielding tensor [17]:[19]

$$\delta_{ij} = \left\langle \Psi^{(0)} \left| \frac{\partial^2 \hat{H}}{\partial B_i . \partial m_j} \right| \Psi^{(0)} \right\rangle + \sum_I \frac{\left\langle \Psi^{(0)} \left| \frac{\partial \hat{H}}{\partial B_i} \right| \Psi_I^{(0)} \right\rangle \left\langle \Psi^{(0)} \left| \frac{\partial \hat{H}}{\partial m_j} \right| \Psi_I^{(0)} \right\rangle}{E_0 - E_I} \tag{73}$$

m is a magnetic moment of a given nucleus.
The above mechanism for ab-initio NMR calculation, can be extended for DFT using SOS-DFPT (Sum-Over-States Density Functional Perturbed Theory) [18]. In this theory, the original sum-over-states equation is given by an approximated equation:

$$\Psi^{KS} = \Psi^{KS(0)} + i\mathbf{B}\sum_{\mathbf{I}} \beta_{\mathbf{I}}\mathbf{\Psi_I^{KS}} + \mathcal{O}\left(B^2\right) \tag{74}$$

$$\beta_I = -\frac{1}{2}\frac{\left\langle \Psi^{(0)} \left| \frac{\partial \hat{H}}{\partial B_i} \right| \Psi_I^{(0)} \right\rangle}{\epsilon - \epsilon_I - \triangle E^{xc}}$$

Index "I" goes over unoccupied states, ϵ is a Kohn-Sham energy and $\triangle E^{xc}$ is the exchange correlation energy difference between occupied and unoccupied states. However, as have been pointed out by Bieger [19], the calculation of the nuclear magnetic shielding cannot be mathematically justified within DFT framework. Because in presence of magnetic fields, the bijective projection between ground state electron density and wave-function is lost.
Even though the Hamiltonian of eq. (61) depends on the choice of gauge origin, the current density is gauge invariant. The calculated shielding tensor is independent of gauge origin, as long as equations are solved exactly. This would require using infinite basis set. However because in practice, the orbitals are usually approximated by finite number of Gaussian functions, gauge dependence arises. So one has to consistently choose gauge origin for calculation. For single atom, position of it's nucleus can be chosen, but there is no proper gauge origin for molecules. Gauge dependence problem can be tackled by introducing gauge origin distributed over the molecule. The most popular methods are GIAO (gauge-including orbitals) [20] and IGLO (individual gauge for localized orbitals) [21]. It is however beyond the scope of this work to derive equations for the IGLO and GIAO methods.

[18] in closed shell systems index goes over all doubly occupied degenerate states
[19] summation index I goes over excited states of unperturbed Hamiltonian

3 Thermodynamics of chemical equilibrium

3.1 Thermodynamic state

Classical thermodynamics describes macroscopic systems in equilibrium. In this discipline, equilibrium is defined as a state of interacting systems, where their thermodynamic parameters are constant. The assumption that all systems at a constant volume will eventually reach equilibrium state is sometimes referred to as a "minus first law of thermodynamics."
The first law of thermodynamics defines the internal energy of a macroscopic system. It says, that internal energy of some arbitrary isolated system is constant, and that can be exchanged with other systems by work done by the system, or heat exchanged. For reversible process the law is stated as follows[20]:

$$dU = T.dS - P.dV \tag{75}$$

Where U is energy, T is temperature, P is pressure, V is a volume and S is a entropy of a system. For experiments that involve chemical reactions this definition is not very convenient. First it defines the change of internal energy through volume and entropy. There is no direct experimental way to measure entropy change, and changes of volume due to chemical reactions are sometimes hard to measure. The remedy for this problem is to introduce state function, that will use different variables. For description of chemical reactions the Gibbs free energy is a good choice. It is defined as

$$G = U + PV - TS \tag{76}$$

So it's differential for a reversible process is

$$dG = VdP - SdT \tag{77}$$

So the Gibbs free energy is a state function of temperature and pressure, the two variables that are much easier controlled in a chemistry lab. It will be shown in a next chapter, how this property can be related to a chemical reactions, and also how can be experimentally measured.

3.2 Chemical equilibrium

Chemical equilibrium is a state in which concentrations of all compounds present in a system are constant. If the reaction occurs in fluid state, chemical equilibrium is a result of all chemical reactions being canceled by their reversed reactions. This case is also called dynamic equilibrium[22].
For 1:1 stoichiometry complex formation, the following reaction occurs:

$$H + G \rightleftharpoons HG \tag{78}$$

Where H ="host" , G ="guest" and HG ="host-guest complex".
The association constant K_a is defined as follows:

$$K_a = \frac{[HG]}{[H].[G]} \tag{79}$$

Where the [X] means a concentration of compound "X" at chemical equilibrium.

3.3 Host-guest chemistry

The simple form of Gibbs free energy as was stated in previous chapter applies only to systems of constant number of particles. For systems consisting of more types particles whose numbers change, we need to define one very important property. It is called a chemical potential, and it is defined as a partial molar Gibbs free energy of a given particle type.

$$G = \sum_i \mu_i n_i \tag{80}$$

[20] This is true only if particle numbers are constant, thus we are ignoring any chemical or nuclear processes.

When numbers of particles of a given system are changed under constant temperature and pressure, the chemical potential is equal to:

$$\left(\frac{\partial G}{\partial n_i}\right)_{p,T} = \mu_i \tag{81}$$

because the total differential of Gibbs free energy in terms of it's partial molar chemical potential components is:

$$dG = \sum_i d\mu_i n_i + \sum_i \mu_i dn_i \tag{82}$$

These two equations implies, that if chemical potential of i-th component of a system changes, the other chemical potential components must response to fulfill this relation[21]:

$$d\mu_i = -\sum_j \frac{n_j}{n_i} d\mu_j \tag{83}$$

Now when we have defined Gibbs free energy in terms of chemical reactions, we can also restate our definition of chemical equilibrium.
Chemical reaction shown in equation (78) will be in equilibrium, when $-\frac{d[HG]}{dt} = \frac{d[G]}{dt} = \frac{d[H]}{dt}$.
But we need to relate this microscopic property to some thermodynamic property. We can say, that energy change is a driving force for a reaction to happen[22]. So for a reaction to be in equilibrium, the change of a Gibbs free energy must be constant. It can be elegantly expressed by:

$$\left(\frac{\partial G}{\partial \xi}\right)_{p,T} = 0 \tag{84}$$

ξ is a reaction coordinate defined as $d\xi = \frac{dn_i}{v_i}$ where v_i is a stoichiometric coefficient of an i-th component.
But because of:

$$\left(\frac{\partial G}{\partial \xi}\right)_{p,T} = \sum_i \mu_i v_i \tag{85}$$

we now see, that knowing the stoichiometric coefficients of a reaction, we can relate chemical potentials of a species once the reaction reaches the equilibrium.

$$\sum_i \mu_i v_i = 0 \tag{86}$$

How the association constant K_a, can be used to estimate the Gibbs free energy change of a reaction?
At elementary level, one very crude approximation needs to be done. It is assumed that all reactants and products of a reaction behave as a ideal gas. And now we need to find a link between equilibrium concentrations of a reaction components and their chemical potential. This can be done by expressing chemical potential from a partition function.
In statistical physics, probability for a particle to be in a state with energy E_i with particle count N_j is:

$$p_{ij} = \frac{exp\frac{(-E_i + N_j\mu)}{k_B T}}{\Xi} \tag{87}$$

Where Ξ is a grand canonical partition function, obtained by summing over all possible states and particle counts.

$$\Xi(T, V, \mu) = \sum_{ij} exp\left[-\left(\frac{E_i + N_j\mu}{k_B T}\right)\right] \tag{88}$$

[21] This of course only applies if pressure and temperature during the process is constant.

[22] Actually a force is not very appropriate analogy, because a change in Gibbs free energy do determine the kinetics of a reaction. Thermodynamics says nothing about reaction rates. In general it rather determines whether a given process is possible or not.

Denoting internal energy of a given reaction component by:

$$U = \sum_{ij} E_i.p_{ij} = k_B.T^2 \left(\frac{\partial \ln \Xi}{\partial T}\right)_{V,\mu} \tag{89}$$

The above expression can be exploited when we note that chemical potential can be also expressed as a partial differential of a Helmholtz energy.

$$\left(\frac{\partial A}{\partial n_i}\right)_{T,V} = \mu_i \tag{90}$$

We can exploit this because there exists a simple expression for Helmholtz energy in terms of a partition function[23].

$$A = U - TS = -k_B T.\ln(\Xi) \tag{91}$$

The grand partition function for non interacting indistinguishable particles can be written through partition functions, that can be then expanded through single particle partition functions.

$$\Xi(T,V,\mu) = \sum_j e^{\frac{N_j \mu}{k_B T}} Z(T,V,N_j) = \sum_j \frac{1}{N_j!} e^{\frac{N_j \mu}{k_B T}} Z(T,V,1)^{N_j} \tag{92}$$

factor 1/N! arises from indistinguishability of particles.
Chemical potential can be expressed using Stirling approximation as

$$\mu_i = -k_B T.\ln\left(\frac{Z(T,V,1)}{N}\right) \tag{93}$$

The single particle canonical partition function for an ideal gas changes linearly with volume $Z(T,V,1) = Z(T,0,1) + \mathcal{O}(\mathcal{V})$, and we are working in an ideal gas approximation $P.V = N k_B T$. Therefore a chemical potential for individual reactants in a reaction is:

$$\mu = \mu^\circ + k_B T.\ln(p) \tag{94}$$

p is a partial pressure of a given reactant in a solution, and μ^0 is a chemical potential of a free substance. The key is, that partial molar pressures in a ideal gas approximation can be related to a concentrations. Determining equilibrium concentrations of all reaction components, can be related to the change of it's Gibbs energy.
Because in chemical equilibrium $\left(\frac{\partial G}{\partial \xi}\right)_{p,T} = \sum_i \mu_i v_i = 0$ therefore $\sum_{i=products} v_i \mu_i = \sum_{j=reactants} v_j \mu_j$.
So the molar Gibbs energy change for that reaction is:

$$\triangle G_p = G_p - G_p^\circ = \sum_{\varsigma=components} v_\varsigma \mu_\varsigma^\circ = -RT.\ln\left(\frac{\prod \frac{p_{products}}{p^\circ}}{\prod \frac{p_{reactants}}{p}}\right) \tag{95}$$

G° is the standard Gibbs function of formation, which is a change of Gibbs energy caused by formation of 1 mole of substance in its standard state (1 bar of pressure and 298.15 K) and $p^\circ = 1bar$. This state is a reference state for Gibbs energy change in (eq. 95).
But we are not able to measure partial molar pressures using NMR spectroscopy. So we will define standard state differently. Because in ideal gas approximation, pressure is proportional to concentration if volume and temperature are unchanged, we define standard state of guest and host molecule as $c^\circ = 1mol.dm^{-3}$. Therefore

$$\triangle G_c = G_c - G_c^\circ = \sum_{\varsigma=components} v_\varsigma \mu_\varsigma^\circ = -RT.\ln\left(\frac{\prod \frac{c_{products}}{c^\circ}.\gamma_{products}}{\prod \frac{c_{reactants}}{c^\circ}.\gamma_{reactants}}\right) = -RT.\ln(K_\gamma.K_a) \tag{96}$$

γ are activity coefficients and they arise as deviations from an ideal gas behavior. For dilute solutions activity coefficients are approximated as unity, so:

$$\triangle G_c = -RT.\ln(K_a) \tag{97}$$

[23]The entropy is in statistical physics defined as a $S = k_B ln(\Omega)$. Because Ω is the number of micro-states, for indistinguishable particles using Stirling approximation it can be expressed as:
$S = k_B ln(\prod_i \frac{g_i^{n_i}}{n_i!}) = k_B + \frac{U}{T} + k_B ln(\Xi)$, where g_i is the degeneracy of i-th state and n_i is the number o particles in that state.

3.4 Calculation of thermodynamic properties

The equations that will be outlined below are again going to assume non-interacting particles. It will be also assumed that the first and higher electronic excited states are entirely inaccessible, which is a reasonable approximation for systems with non negligible HOMO-LUMO gap.
The starting point is a partition function, from which we can determine internal energy (eq. 89) and entropy (footnote 23). Once we know this two quantities, Gibbs free energy can be easily calculated.

$$G = U - TS + k_B T \tag{98}$$

Remember that we are working with an ideal gas approximation.
The task is now to determine the partition function. For clarity we can broke it into 4 parts: translational, vibrational, rotational and electronic.
Translational partition function of an ideal gas has the form:

$$Z_{trans}\left(T, V, 1\right) = \frac{k_B T}{P}\left(\frac{2\pi m k_B T}{h^2}\right)^{\frac{3}{2}} \tag{99}$$

Because the excited states are assumed to be inaccessible at any temperature and the energy of the ground state is set to be zero, electronic partition function takes the form:

$$Z_{elec}\left(T, V, 1\right) = \left(2S + 1\right) e^{-\frac{E_g}{k_B T}} \tag{100}$$

S is a spin multiplicity and E_g is a ground state electronic energy.
Rotational partition function for a nonlinear polyatomic molecule is

$$Z_{rot}\left(T, V, 1\right) = \frac{\sqrt{2 I_x I_y I_z}}{\sigma}\left(\frac{2 k_B T}{\hbar^2}\right)^{\frac{3}{2}} \tag{101}$$

I are principal moments of inertia, and σ is the number of rotations that will turn the molecule into itself.
The contributions to partition function from vibrational motion of the molecule, is given as a product of each normal vibrational mode:

$$Z_{vib}\left(T, V, 1\right) = \prod_{i}^{3N-6} \frac{e^{-\frac{\hbar \varpi_i}{2 k_B T}}}{1 - e^{-\frac{\hbar \varpi_i}{k_B T}}} \tag{102}$$

And partition function is now simply obtained as a product of all its constituents

$$Z = Z_{elec}.Z_{trans}.Z_{rot}.Z_{vib}$$

Equations discussed above can be found in "Molecular Thermodynamics" by McQuarrie and Simon, chapter 17 [23].

4 Chirality sensing with NMR

4.1 Stereoisomerism and Chirality

Stereoisomers are molecules with identical molecular formulas, identical molecular sequences but different spatial orientations of their constituent atoms in space. If two stereoisomers are mirror images of each other, we call them enantiomers. The ability of molecule to have enantiomers is called chirality, and is usually result of a tetrahedral atom with four different groups attached to it, also called a chiral center. Of special interest are molecules with only one chiral center, because in this case a pair of enantiomers is related to one another with parity operation. Chemical properties of matter are dictated by electromagnetic interactions. Because Maxwell's equations are invariant under parity operation, the two enantiomers have identical chemical properties[24],

[24] Because weak interactions unlike gravitation, strong interactions and electromagnetism break parity conservation, the two enantiomers do not have identical chemical properties. However their effect on chemical properties is small, and have not been yet verified experimentally.

except for the direction in which they rotate polarized light and how they interact with other chiral molecules. If enantiomers are optically active, they rotate polarized light in opposite direction. However because rotation of polarized light is additive, the experimentally determined value depends on enantiomeric purity. But even enantiomeric purity can't be straightforwardly determined, because optical purity and enantiomeric purity are not necessarily equivalent and can exhibit non linear dependence[24].
However because amino-acids, carbohydrates, hormones and many other biomolecules are chiral, biological systems with enormous amounts of homochiral compounds is very sensitive to chirality. Interaction between some enantiomer molecule and receptor could be chiral dependent. It is a lock and key mechanism. Thus each enantiomer could be metabolized by different pathway, resulting in a different reaction kinetics or even different products, therefore different pharmacological activity. In pharmaceutical industries, 56% of the drugs currently in use are chiral and 88% of those are marketed as racemates[25].

4.2 Using chiral reagents as a chirality sensors

Besides traditional chiroptical methods there also exist other methods to determine enantiomeric excess. They are based on a interaction with some other chiral substances. Chromatography using chiral stationary phase is a one way to promote chiral separation.
Even though in NMR spectroscopy respective enantiomers can't be distinguished in an achiral medium. When their interaction with some chiral molecule is promoted, and enantiomers are thus complexed into a diastereoisomers, the resulting spectroscopic properties of diastereomeric complexes are different. There are two basic types of chiral agents used. Chiral derivatizing agents that react with the analyzed enantiomers through covalent bonds[26] and chiral solvating agents interacting through noncovalent, intermolecular forces[27].

4.3 Achiral sensors of chirality

4.3.1 Porphirinogens

Porphirine is a tetrapyrrole molecule. It is composed of four pyrrole rings, connected by sp^2 hybridized carbon atoms. Because of sp^2 carbons, the core is planar, which results to following fully conjugated structure (figure 1).

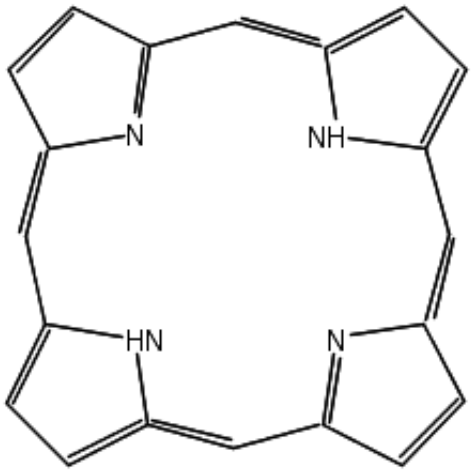

Figure 1: conjugated structure of tetrapyrrole macrocycle

The nitrogen atoms are within the inner core, and are able to complex with metal ions[28]. The carbons that connect pyrrole molecules are called meso atoms, and outer pyrrole carbons are called β carbons.
There are many structural modifications of porphirine macrocycle. The porphirines, where the modification is done by attaching substituents on meso carbon are called porphirinogens. In most porphirinogens, the conjugation is also modified. This results into modification of the por-

phyrin skeleton, and planarity is lost. One interesting porphirinogen of this type, reported first by Milgrom and his coworkers[29] is oxo-cyclohexadienylidene porphyrinogen, where the meso substituents are oxocyclohexadiensalkylates with tert-butyles for better solubility on non-polar solvents. The resulting molecule is meso-tetrakis 3,5-di-tert-butyl-4-oxo-2,5-cyclohexadienylidene porphyrinogen (OxP) (figure 2). This modifications also increases their potential a binding agents to non-metallic compounds[30]. Milgrom and his coworkers also found, that N-alkylation of tetrapyrrole ring is a useful way of stabilizing the structure of the compounds against protonation[31]. Also the redox and spectral properties of the compounds are tunable by altering N-substituents[32]. The molecule that we studied, had two brombenzene N-substituents at adjacent pyrroles. The structure of N21,N23-Di-brombenzene-3,5-di-tert-butyl-4-oxo-2,5-cyclohexadienylidene porphyrinogen (DiBrBzOxP) is shown below (figure 2).

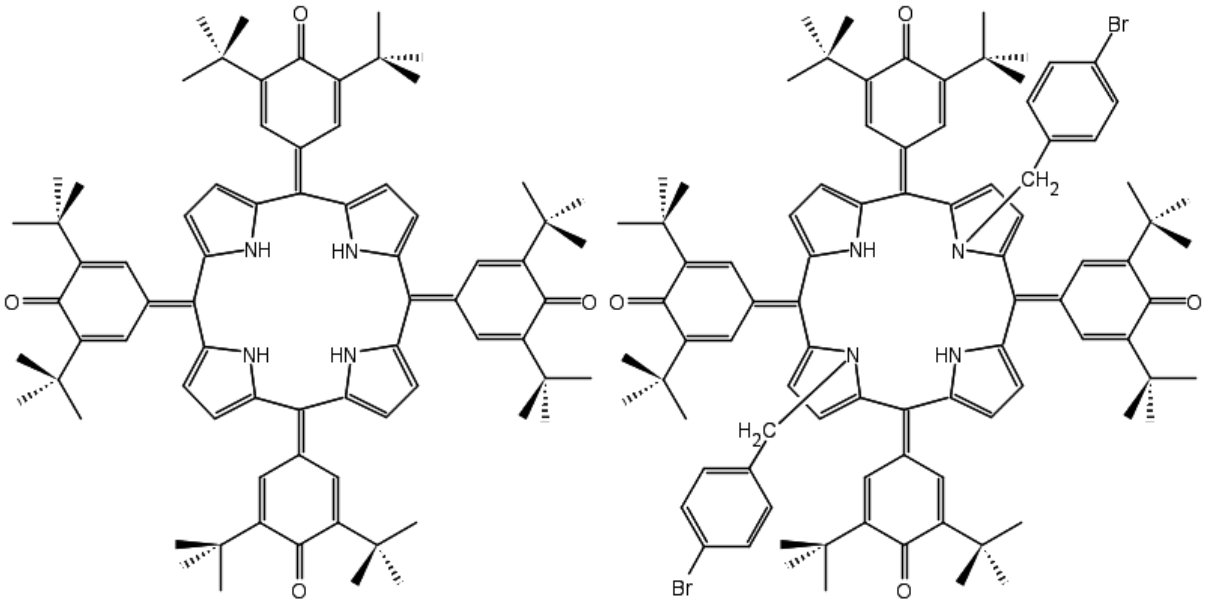

Figure 2: *Structure of meso-tetrakis 3,5-di-tert-butyl-4-oxo-2,5-cyclohexadienylidene porphyrinogen (OxP) on the left. And on the right side it's N-brombenzenated form.*

Also the crystallization of OxP is mediated by water molecules. There is a H-bonding between tetrapyrrole N-H and the water oxygen atom. This leads to formation of a layered crystallic structure. Crystal packing of the N-alkylated porphyrinogens isn't mediated by any hydrogen-bonds interactions. Because there are no short contact distances, the hydrogen bonding or other short range forces are not apparent[33]. The absence of layered crystalic structure also leads to faster solvation.

4.3.2 NMR sensing of chirality with porphirinogens

Until recently NMR spectroscopic detection of guest chirality using an achiral host was not possible. It is because NMR is based on either chiral discrimination by the host or diastereomeric host guest complex. For both methods chiral sensor is necessary[34]. However recently the first instance of chiral information detection, by signaling from an achiral host, in NMR spectroscopy was reported[35]. Oxoporphyrinogen (figure 2) have been used as a host, because it can bind guests with pyrrolic NH groups. As a guest a chiral mandelic acid have been used.

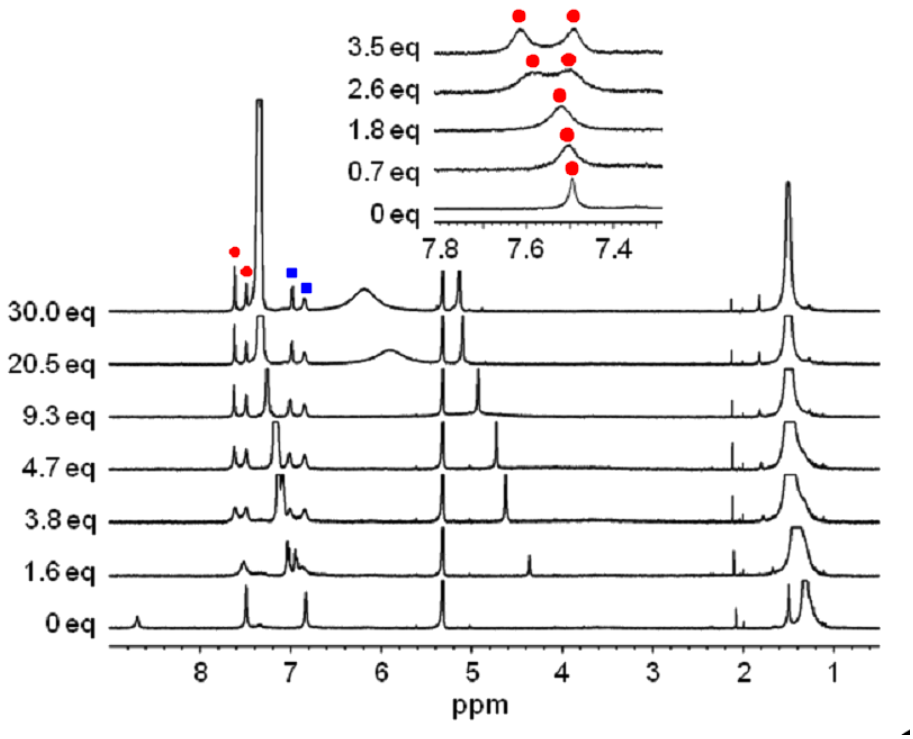

Figure 3: *^{1}H-NMR titration of OxP with R-mandelic acid performed in CD_2Cl_2 at 25 °C. [33]*

Addition of racemic mandelic acid resulted in ^{1}H-NMR downfield shifts of quinonoid protons, tert-butylic protons, pyrrolic β-protons and NH protons (figure 3). The shifts were increasing gradually with the amount of guest added. This changes in ^{1}H-NMR spectra of OxP can be associates with a formation of host-guest complex with fast chemical exchange between complexed host-guest state and a standalone OxP state. For pure enantiomer, quinonoid protons and β-protons on pyrrole signals also split into two peaks each. But the rest of the spectra remains the same. When racemic and nonracemic mixtures of mandelic acid were used in this system, peak separations changed linearly with enantiomeric excess (figure 4).

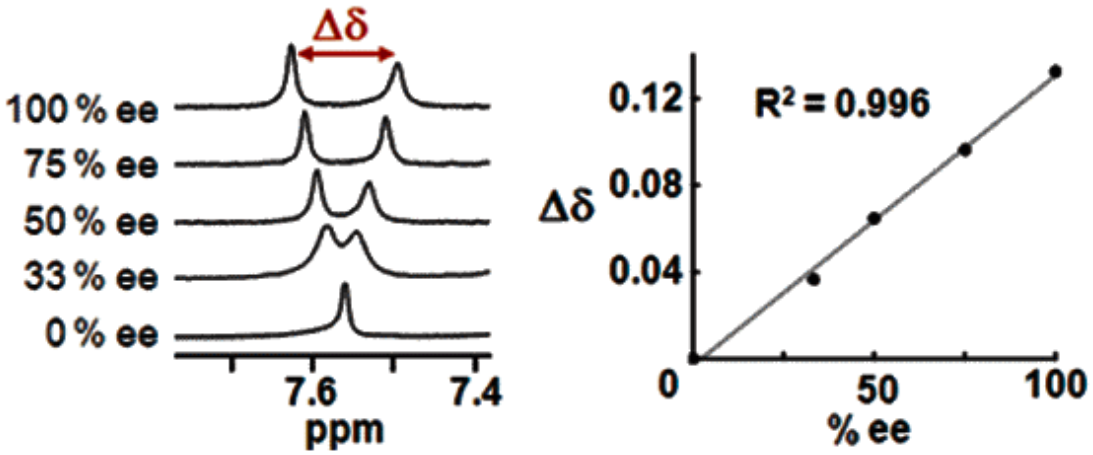

Figure 4: *Partial ^{1}H NMR spectra of OxP in the presence of mandelic acid with various enantiomeric excess values, % ee (left). Correlation between differences in chemical shielding of quinonoid proton peaks and the enantiomeric excess values (right) [33].*

They have also confirmed the complexation of OxP with mandelic acid by UV/vis titration. During the addition of mandelic acid into the solution of OxP, graduate increase of absorption band at 789 nm accompanied with intensity decrease of Soret-type band at blue part of visible spectra, with isosbestic points at 357 and 643 nm (figure 5). From UV/vis titration, Job's plot

was also constructed, and formation of a 1:2 complex[25] was concluded. The UV/vis titration gives identical results with racemat or enantiomeric mandelic acid.
Adding methanesulfonic acid into a CH_2Cl_2 solution of OxP, resulted into similar UV/vis spectra changes. In low temperature ^{1}H-NMR spectra of CD_2Cl_2 solution of OxP with mandelic acid the tert-butyl peak gradually split into two peaks and a new peak appeared at 6.49 ppm (figure 6). And also in FT-IR spectroscopy OH band at 3602 cm^{-1} appeared during titration. These changes suggest a protonation of OxP.

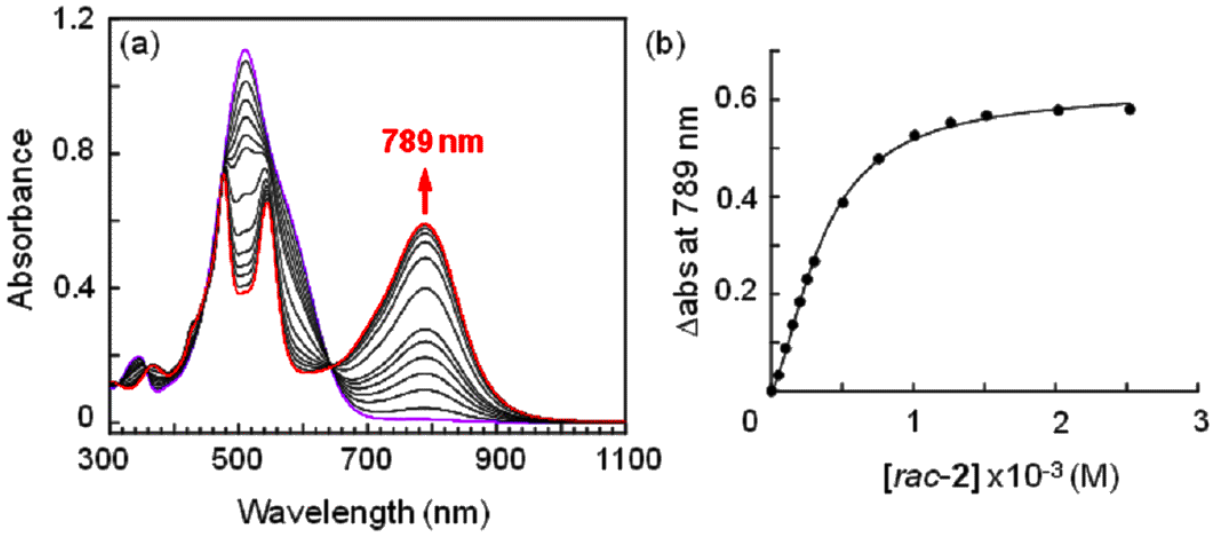

Figure 5: *UV/vis spectral changes observed during titration of OxP with R-mandelic acid performed in CD_2Cl_2 at 25 °C [33]*

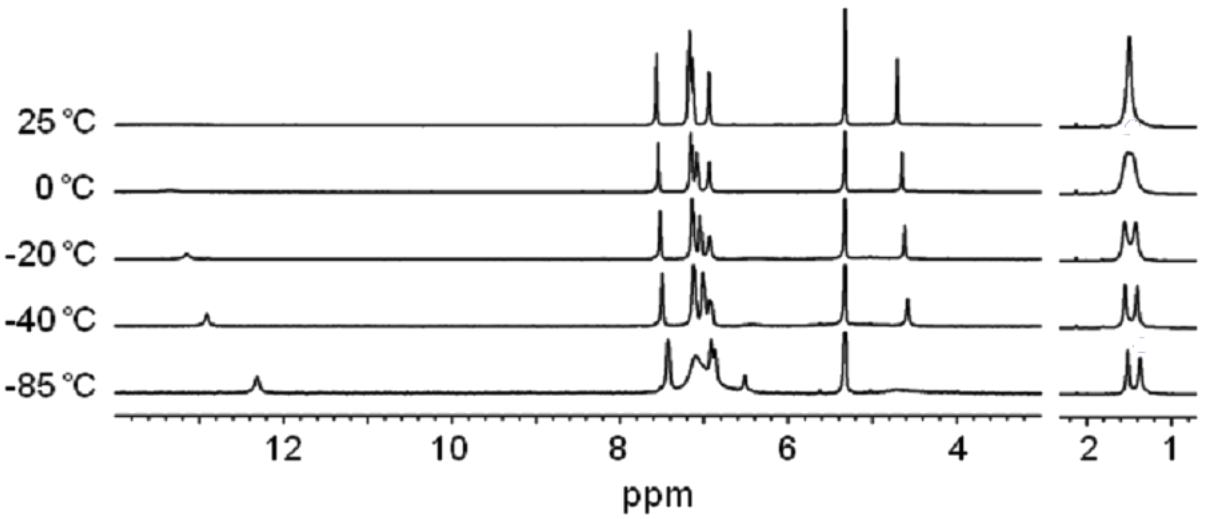

Figure 6: *^{1}H-NMR spectra of OxP in the presence of 5.3 equivalents of racemic mandelic acid with various temperatures (in CD_2Cl_2)[33].*

For our experiment, we have chosen brom-benzylated version of OxP (figure 2), that should have better solubility in organic solvents and be more resistant against protonation. We also predicted that stoichiometry should be 1:1, that will simplify the complex formation and allow clearer interpretations. Better stability against protonation will allow us to study effect of porphirinogen protonation to guest-complex formation. For a guest molecule we have chosen ibuprofen (figure 7), because it is a chiral carboxylic acid with chirality dependent metabolic properties in humans. Determination of it's enantiomeric excess thus could serve for studies of its metabolism. The complex will be also studied from a computational perspective, in order to better understand its physical aspects.

[25] host:guest

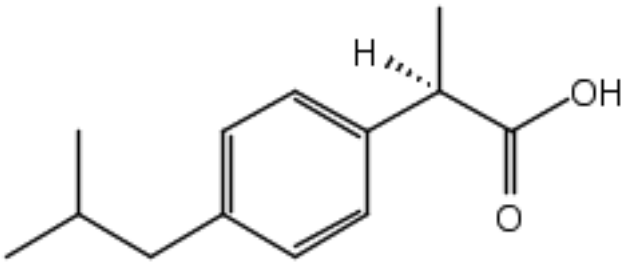

Figure 7: *S-Ibuprofen*

5 Determination of association constant

Very important property for any non-covalent complex is it's association constant, as by knowing the association constant, one can solve for the Gibbs free energy of the reaction. Because we are dealing with reactions that occur at constant pressure and temperature, Gibbs free energy is the property that quantitatively describes formation of a complex. It can be determined using a number of experimental methods. The most widely used is NMR titration, in which variation of some NMR parameter against molar ratio change of reaction components is determined and analyzed.

5.1 NMR titration

The NMR spectra for a given concentration of host and guest molecules, depend on association constant and the rate at which formation of complex occurs. For fast chemical exchange[26], any observed chemical shift $\delta_{observed}$ is a weighted average of shifts in free δ_H and complexed δ_{HG} molecule.

$$\delta_{observed} = \frac{[G]\delta_H + [HG]\delta_{HG}}{([G] + [HG])} \tag{103}$$

If the complex formation is fast enough to adhese signals at δ_G and δ_{HG}, but not sufficiently fast to fully average them, equation (103) is not valid anymore. $\delta_{observed}$ can be shifted towards the position of the signal corresponding to more populated form, which then leads to lower values of association constant and Gibbs free energy of complex formation[36].

5.2 Graphical methods

One of the most widely used techniques for measuring association constants is NMR spectroscopy. NMR spectroscopy can also provide structural information about studied complexes. One way, how to use a relationship (103) to determine the association constant for 1:1 stoichiometry are linearization methods. These methods always try to find an approximate linear relationship between observed chemical shift and concentrations of compounds. Because of approximations they require measurements in the presence of a large excess of one of the reagents, which is sometimes difficult to achieve. A further limitation is, that they are extrapolated to a regions of high host concentrations, which introduces an error for weak complexes. Their advantage is simplicity, that can be interpreted graphically. The most common methods are double reciprocal, Scatchard or Rose-Drago method[37].

5.3 Curve fitting methods

Nonlinear curve fitting methods require no approximations and are not limited to 1:1 stoichiometry. Using modern computers they have became routine today. We will first derive the equation that relates observed chemical shift to the titrated amount of guest.

[26] Noncovalent bonds in fluid phase are not stable, they are constantly created and destroyed. If the exchange rate is larger than the Larmor angular frequency difference of the observed resonances in two states, then the fast chemical exchange occurs.

Assigning the total concentrations of [H] and [G] as $[H]_t$ and $[G]_t$ respectively:

$$[H]_t = [H] + [HG] \tag{104}$$

$$[G]_t = [G] + [HG] \tag{105}$$

we are looking for equation in following form:

$$\delta_{observed} = \frac{[H]}{[H]_t}\delta_H + \left(1 - \frac{[H]}{[H]_t}\right)\delta_{HG} = f\left([G]_t\right) \tag{106}$$

Titration is usually done that host concentration is unchanged, while the total concentration of guest is varied. So we need to express [H] as a function of $[G]_t$ and some variables that will be constant during titration. To achieve this some algebra needs to be done. Equations (79,104 and 105) are set of 3 linear equations with 6 variables. We can thus eliminate this set into one equation of 4 variables. $[H]_t$ is known and K_a is what needs to be determined, and will therefore serve as a parameter during curve fitting. So we have chosen to eliminate [HG] and [G] from the equations. This can be done by following straightforward procedure.
First equation (79) is rearranged to define [HG] and then used to substitute for [HG] into equation (104), which is then rearranged into:

$$[G] = \frac{[G]_t}{(1 + K_a.[H])} \tag{107}$$

Equation (107) is now plugged into equation (79)

$$K_a = \frac{[HG].\,(1 + K_a.[H])}{[G]_t.[H]} \tag{108}$$

Now we substitute for [HG] with eq. (105)

$$K_a = \frac{([H]_t - [H])\,.\,(1 + K_a.[H])}{[G]_t.[H]} \tag{109}$$

[G] can be expressed as a argument of second order polynomial equation.

$$K_a.[H]^2 + (1 + K_a.\,([G]_t - [H]_t))\,[H] - [H]_t = 0 \tag{110}$$

And finally expressing root of eq. (110), will define [G] through parameter K_a and measurable values $[H]_t$ and $[G]_t$

$$[H] = \frac{-1 - K_a.\,([G]_t - [H]_t) + \sqrt{(1 + K_a.\,([G]_t - [H]_t))^2 + 4.K_a.[H]_t}}{2.K_a} \tag{111}$$

$[G]_t$will serve as a argument of a titration fit. δ_H will be determined experimentally by measuring the ^{1}H-NMR spectra of pure host molecule. $[H]_t$ will be measured, by weighting the amount of host dissolved in a solvent. δ_H and K_a will serve as a parameters for a titration.

6 Experiment

6.1 Chemicals and apparatus

Crystallic form of di-brombenzene-oxo-porphyrinogen (DiBrBzOxP) was supplied by National Institute for Materials Science, Tsukuba, Japan. Deuterochloroform with 0.03% volume of tetramethylsilane stabilized by silver foil and trifluoroacetic acid were purchased from Sigma-Aldrich Co. S-ibuprofen from TCI Co. Ltd. and racemic ibuprofen from TCI Co. Ltd. DiBrBzOxP and ibuprofen were dehydrated in low pressure dryer for 24 hours at 0.1atm and 50°C. Deuterochloroform was dehydrated with 4Å pore size molecular sieves. ^{1}H-NMR spectrum were obtained with Bruker Avance 500MHZ spectrometer using TBI probe. A single pulse acquisition followed by acquisition of the spectra was used. Length of $\frac{\pi}{2}$ pulse was 0.0115 ms, and the delay that

allowed magnetization to return to its equilibrium state was 5 s. Sequence was repeated 32 times, until desired signal to noise ratio was obtained. The resulting FID was then transformed using Fast Fourier Transform algorithm from time to frequency domain, and phases of all spectra were corrected manually. TMS (Tetramethylsilane) signal was set to be 0 ppm. NMR temperature calibration was performed using a standard sample of 100% methanol and the calibration equation[38].
Raman spectra presented were excited with the 532 nm laser (5mw on the sample) and collected in the 90° scattering geometry using spectrograph (Jobin Yvon–Spex 270 M) equipped with a notch filter to reject Rayleigh scattering and CCD detector with 1340 pixels in spectral axis. The samples were placed into 1cm quartz cell and resulting signal was obtained under 6x10 sec. exposures.
UV/vis spectra were recorded on Perkin-Elmer spectrometer where light was generated with high-pressure deuterium discharge tube and halogen lamp. Transmitted light was recorded in 1nm steps. Because spectra were recorded simultaneously with Raman spectra, same 1cm quartz cell was used. Detailed description of SVD (singular value decomposition) that was performed can be found in[39].

6.2 Results

6.2.1 Guest NMR titration

Chemical shifts of all NMR signals were obtained by Lorentz-curve least-square iterative fitting with Origin 8.1 using Levenberg–Marquardt algorithm. Second order J-coupled signals of β-protons were fitted according to results obtained in section 1.6. I will keep already proposed letter convention, where $\Delta(ppm)$ is difference in chemical shielding of J-coupled β-protons and $\delta(ppm)$ is their average chemical shift (figure 9). Binding isotherms were fitted by least-squares iterative analysis using an in-house written FORTRAN routine based on simplex algorithm, where real root of cubic polynomial was found using bisection method (figures 14 and 15).
For the experiment the solution of DiBrBzOxP in deuterochloroform with concentration $1g/mol$ or $0.00068mol/l$ was prepared. To ensure complete dissolution of DiBrBzOxP, the sample was heated to $50°C$ and placed into ultrasound chamber for 2 minutes[27]. For titration we made another sample with same DiBrBzOxP concentration, but with addition of 1612 molar equivalents of S-Ibuprofen. The molar equivalent of S-Ibuprofen was determined by integration of non overlapping ^{1}H signals (4.42ppm peak of DiBrBzOxP with CH-quartet proton of S-Ibuprofen at 3.70-3.75ppm). During the titration ^{1}H-NMR spectrum every different mixture of DiBrBzOxP with S-Ibuprofen were recorded. The spectrum of pure DiBrBzOxP is shown on figure 8.

[27] This procedure was used for all measurements in this work.

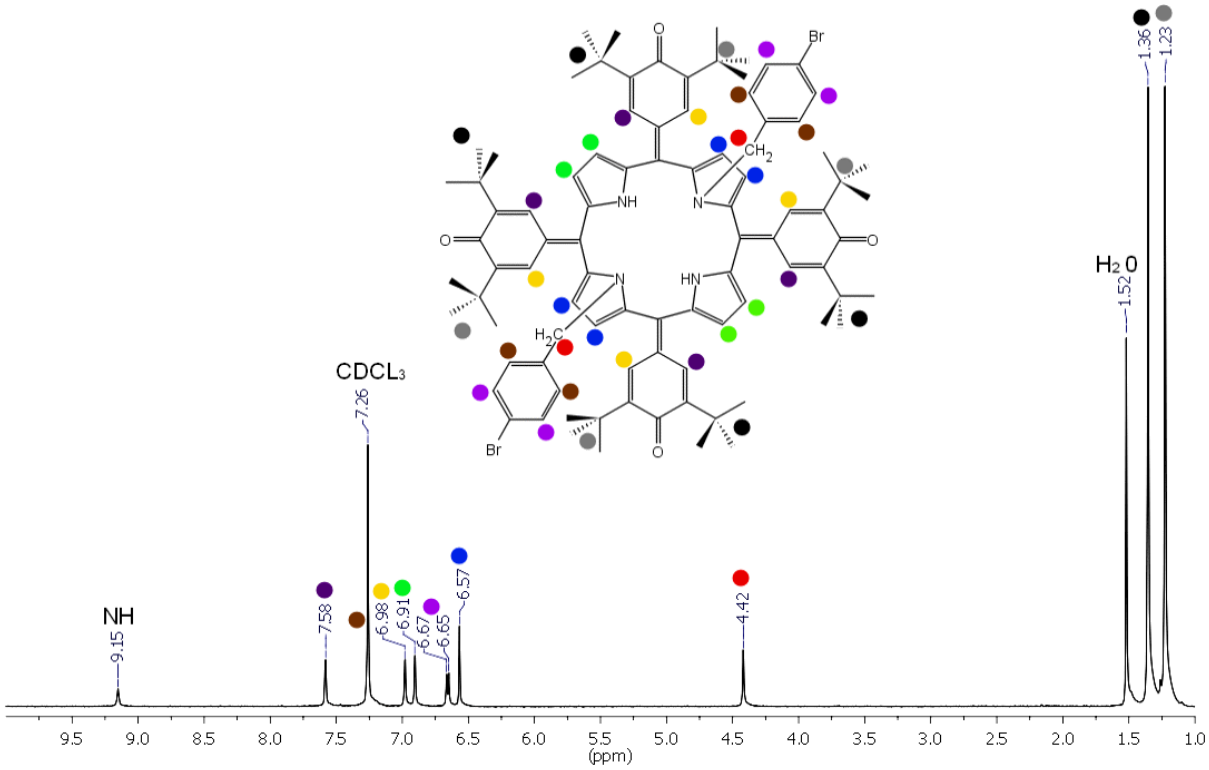

Figure 8: *^{1}H-NMR spectrum of DiBrBzOxP (0.00068mol/l, $CDCl_3$, 25°C). All signals were assigned with COSY NMR sequence.*

The addition of S-Ibuprofen resulted in upfield[28] shift of pyrrole β-protons (figure 10). Because original signal disappears, and the position of new signal changes gradually with S-Ibuprofen added, we concluded a fast chemical exchange between complexed and non-complexed host. For R-enantiomer signal also gradually splits indicating a characteristic scalar J-coupling, which means that the β-protons on a same pyrrole ring loose their magnetic equivalence if a complex is formed. This indicates that the two β-protons on a same pyrrole ring, which are equivalent in DiBrBzOxP molecule are asymmetrically shielded in complex. If a racemic form of ibuprofen is added, the upfield shift persist but the scalar J-coupling disappears. So we concluded that S-enantiomer shields the β-protons in opposite order and fast chemical exchange average out the arising asymmetry. This dynamics allows for determination of enantiomer abundance, because if concentration of guest is unchanged, and different ratios of R:S of guest are used, observed chemical shift difference of the β-protons depends linearly on enantiomeric excess (figure 11).

[28] Term upfield refers to low ppm values and vice versa.

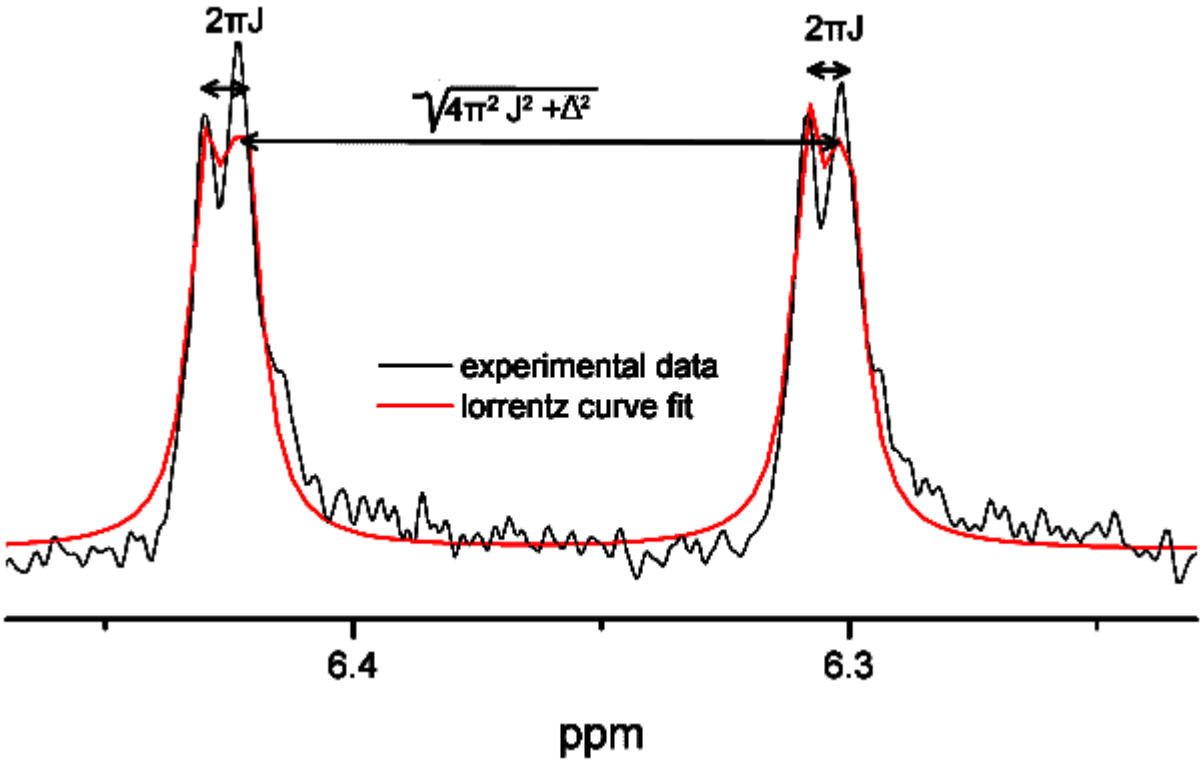

Figure 9: *Partial* ^1H *NMR spectra of DiBrBzOxP (0.00068mol/l,* $CDCl_3$*, 25°C) in the presence of 250 molar equivalents of ibuprofen and corresponding Lorentz-curve with parameters* $\triangle = 0.12ppm$*, J=3.8Hz and* $\delta = 6.37ppm$*. Coefficient of determination is 0.997*

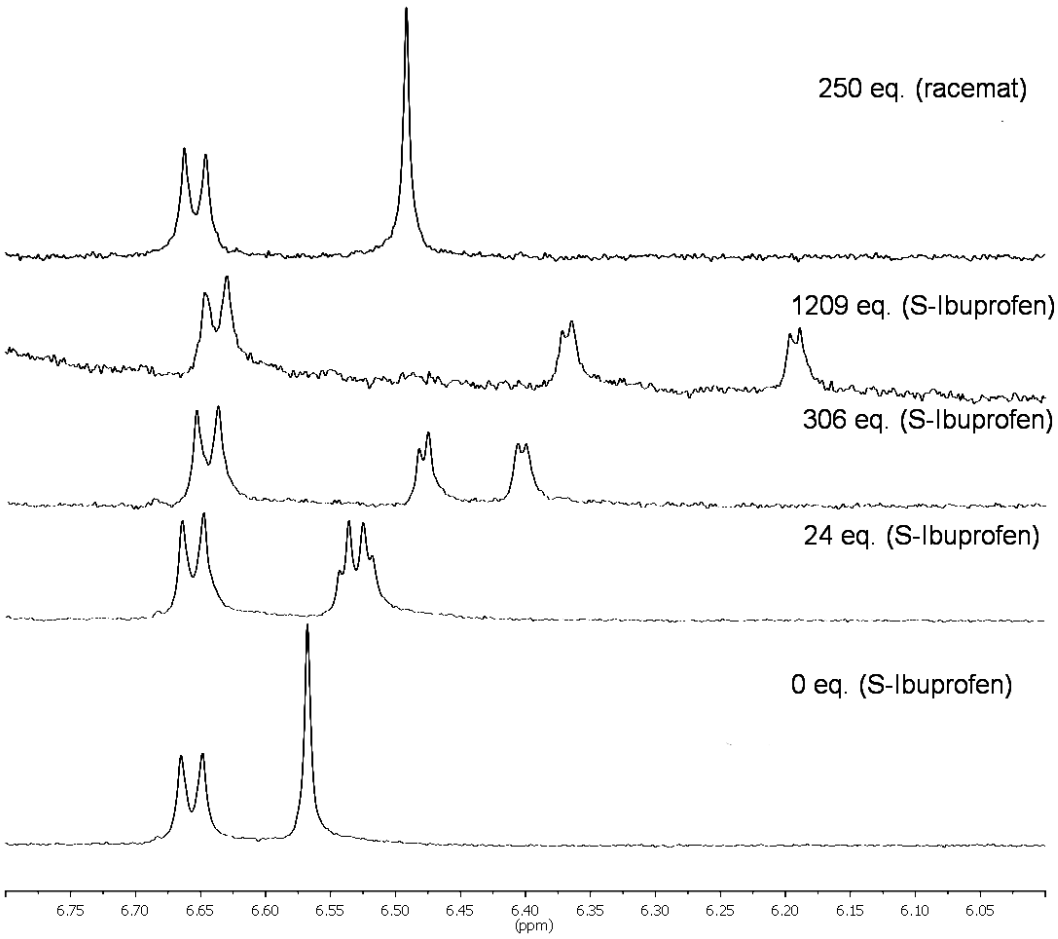

Figure 10: *Partial*^{1}*H-NMR spectrum of DiBrBzOxP with different amounts of S or racemic Ibuprofen added (0.00068mol/l,* $CDCl_3$*, 25°C). Molar equivalents are referred to DiBrBzOxP.*

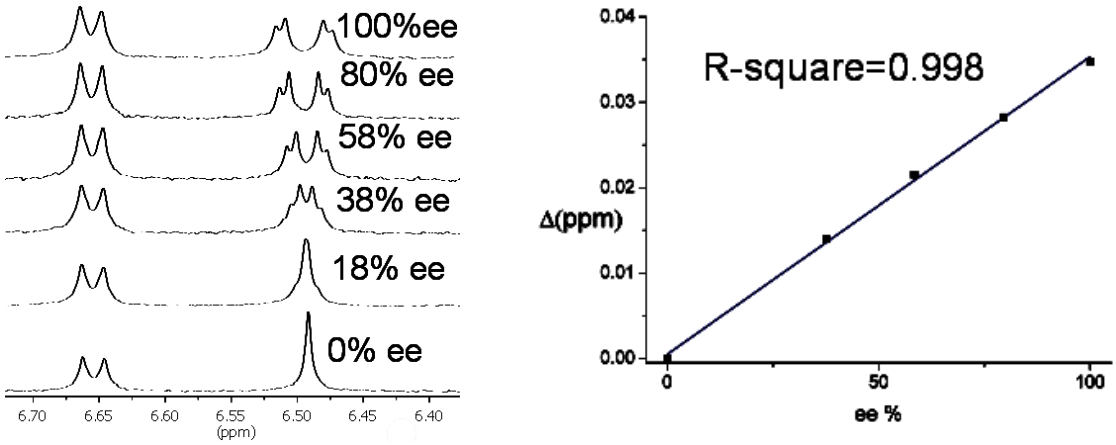

Figure 11: *Partial ^1H NMR spectra of DiBrBzOxP (0.00068mol/l, $CDCl_3$, 25°C) in the presence of 250 molar equivalents of ibuprofen having various enantiomeric excess values, % ee (left). Linearly fitted correlation between difference in chemical shift of β-protons and enantiomeric excess (right).*

6.2.2 Competitive inhibition by water

There is one more change in DiBrBzOxP spectrum that was observed due to titration[29]. NH protons also shift gradually to higher ppm (figure 12). This means that complex formation involves NH protons. Our suggestion was that carboxyl group of ibuprofen binds to NH groups of DiBrBzOxP with hydrogen bonds. However the behavior of NH protons shift does not correlate with changes on β-protons.This can be explained by complexation with another molecule, most probably water.

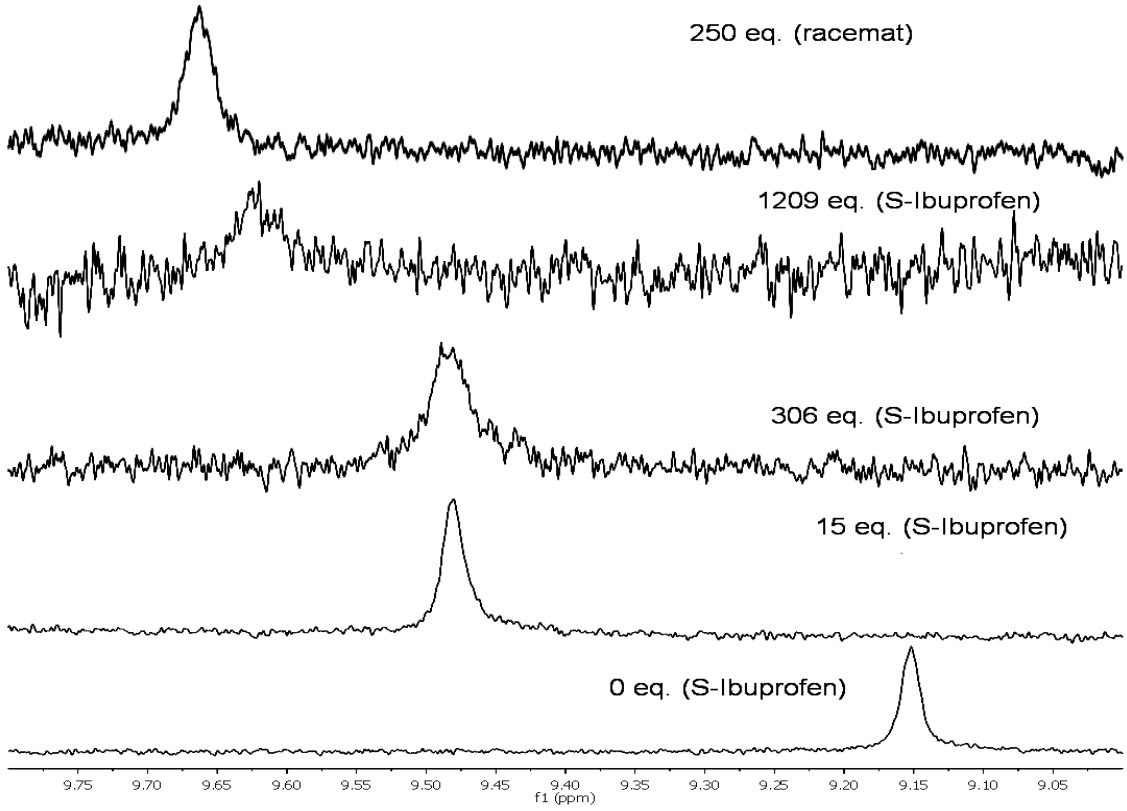

Figure 12: *Partial^{1}H-NMR spectrum of DiBrBzOxP with different amounts of S or racemic Ibuprofen added (0.00068mol/l, $CDCl_3$, 25°C).*

[29]Other signals either remain unchanged due to complex formation, or overlap with ibuprofen peaks.

The complexation with water, would also cause competitive inhibition to complex of DiBrBzOxP with ibuprofen. To confirm this hypothesis, we titrated solution of DiBrBzOxP with S-Ibuprofen using deionized water (figure 13). When water was added the NH signals are shifted downfield, and β-proton signals are also shifted downfield and their difference in shielding is reduced. This clearly confirms the hypothesis, that water molecules bind to NH protons of DiBrBzOxP and cause competitive inhibition to ibuprofen complex.

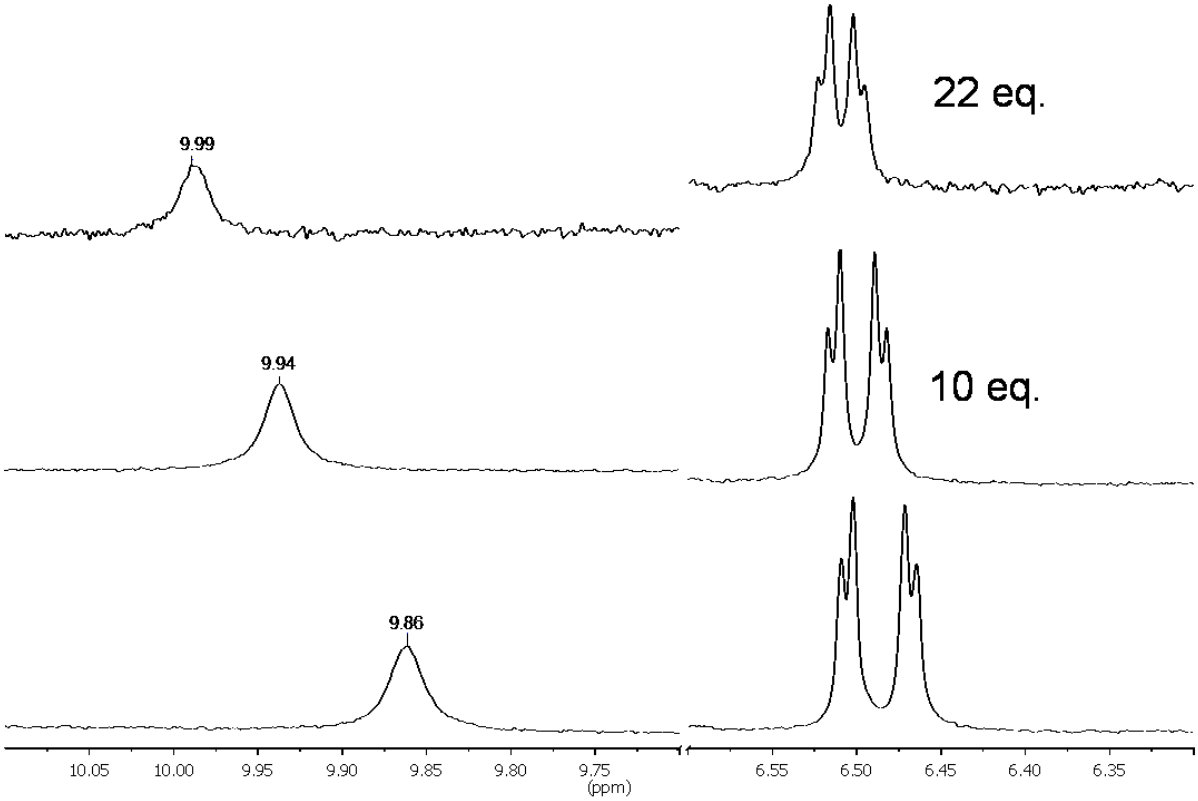

Figure 13: Partial ^1H NMR spectra of DiBrBzOxP (0.00068mol/l, $CDCl_3$, 25°C) in the presence of 160 molar equivalents of S-Ibuprofen with different amounts of water added.

To correctly calculate association constant the competitive inhibition of water must have been considered. The method described in section 5.1.3 is modified to take water inhibition into account. Equation 78 now has the form

$$HG \underset{-G}{\overset{K_G}{\underset{+G}{\rightleftharpoons}}} H \underset{-W}{\overset{K_W}{\underset{+W}{\rightleftharpoons}}} HW \tag{112}$$

If the tedious but straightforward procedure outlined in section 5.3 for above reaction is repeated, the host concentration can be expressed as a solution of this cubic equation[30]:

$$K_G K_W [H]^3 + [K_G + K_G + K_G K_W ([W]_t + [G]_t - [H]_t)][H]^2 + [1 + K_G([G]_t - [H]_t) + K_W([W]_t - [H]_t)][H] = [H]_t \tag{113}$$

The concentration of water can be easily found by integrating respective signal in ^{1}H-NMR spectrum, and its equilibrium constant need to be determined. The equilibrium constant K_W was determined by titration of DiBrBzOxP with water. 1:1 binding isotherm was constructed by least-square three parameter fit. We fit chemical shift of NH protons as a function of molar water equivalents (section 5.1.3).

[30]Because closed solution for cubic equation is complicated, during the curve fitting process the free host concentration was determined iteratively using bisection method.

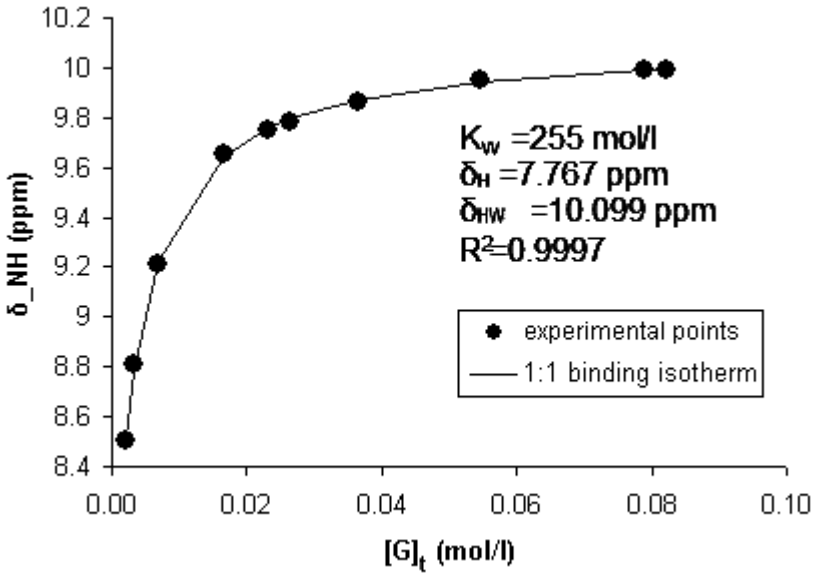

Figure 14: *1:1 fitted binding isotherm of* ^{1}*H-NMR spectrum of DiBrBzOxP titrated by water (0.00044mol/l, CDCl*$_3$*, 25° C)*

The coefficient of determination is good enough to confirm that water binds at 1:1 stoichiometry. And also downfield shift due to complex formation agrees with earlier titrations (figure 13). This binding constant was used for DiBrBzOxP-water complex $K_W = 255$. The amount of water in solution of DiBrBzOxP in deuterochloroform was 7 molar equivalents. We were not able to determine amount of water after S-Ibuprofen was added, because the ^{1}H-NMR signal of water was covered with signal from S-Ibuprofen. So it was assumed that amount of water in solution remained constant after addition of S-Ibuprofen. Because β-proton ^{1}H-NMR shift remained constant, the binding isotherm for S-Ibuprofen titration has the same form as one proposed in section 5.1.3. Only difference is that equation 105 must be substituted with equation 108.

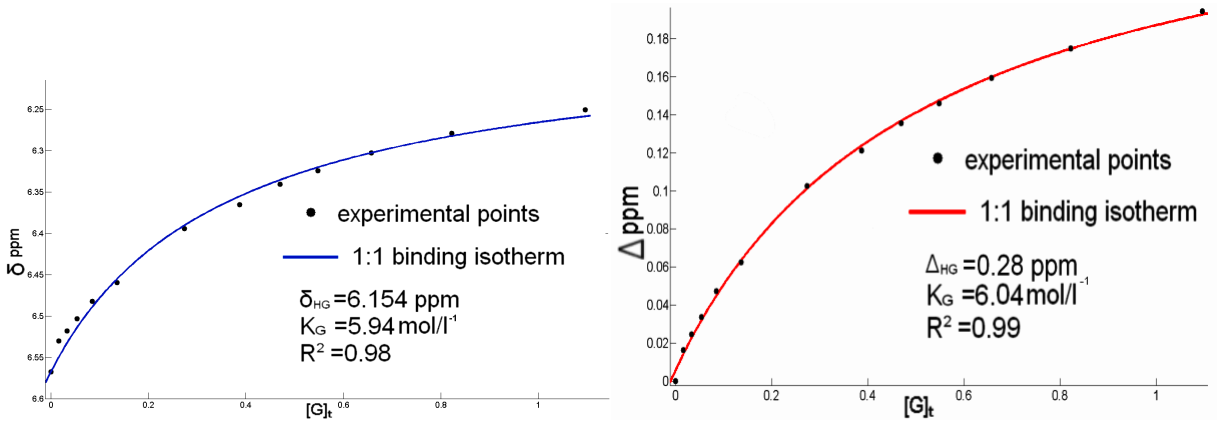

Figure 15: *1:1 fitted binding isotherms of averaged* ^{1}*H-NMR* β*-pyrrole shifts* δ **(left)** *and of chemical shift difference* Δ **(right),** *for DiBrBzOxP titrated by S-Ibuprofen (0.00068mol/l, CDCl*$_3$*, 25° C)*

Binding isotherms of β-pyrrole shifts δ and their chemical shift difference Δ against S-Ibuprofen concentration gave both very similar values for association constants (figure 15). Coefficient of determination for β-pyrrole shifts δ fit is not very good (0.98), and most distant points from fitted curve are points that have been measured due to end of experiment. We therefore concluded, that there must be some other process that was omitted in our analysis. The most crude approximation was, that water concentration remained constant. In figure 16 there is plot of ^{1}H-NMR NH signals for same titration. NH protons signals, unlike β-pyrrole protons signals sense DiBrBzOxP-water complex. Because NH signals, that also have different chemical shift

in complex, do not follow the same trend as β-pyrrole signals, we concluded that amount of water varied during titration. On figure 16 we see, that as 1612 eq. solution was diluted with 0 eq. solution the NH signals were not following the same trend as β-pyrroles, and to the end of titration they even shifted in a opposite direction, indicating that amount of DiBrBzOxP-water complex was increasing. Note that lower eq. solutions were measured later in time. The source of water was probably vapor that entered the sample during manipulation with solutions. This introduced an error into determination of association constant.
Using $K_G = 6.02(mol/l)^{-1}$ and (equation 97) we have determined Gibbs free energy of complex formation. The value is $\Delta G = 4.44kj/mol$. The real value is probably higher because our model assumes lower amounts of water during titration, therefore competitive inhibition is underestimated.

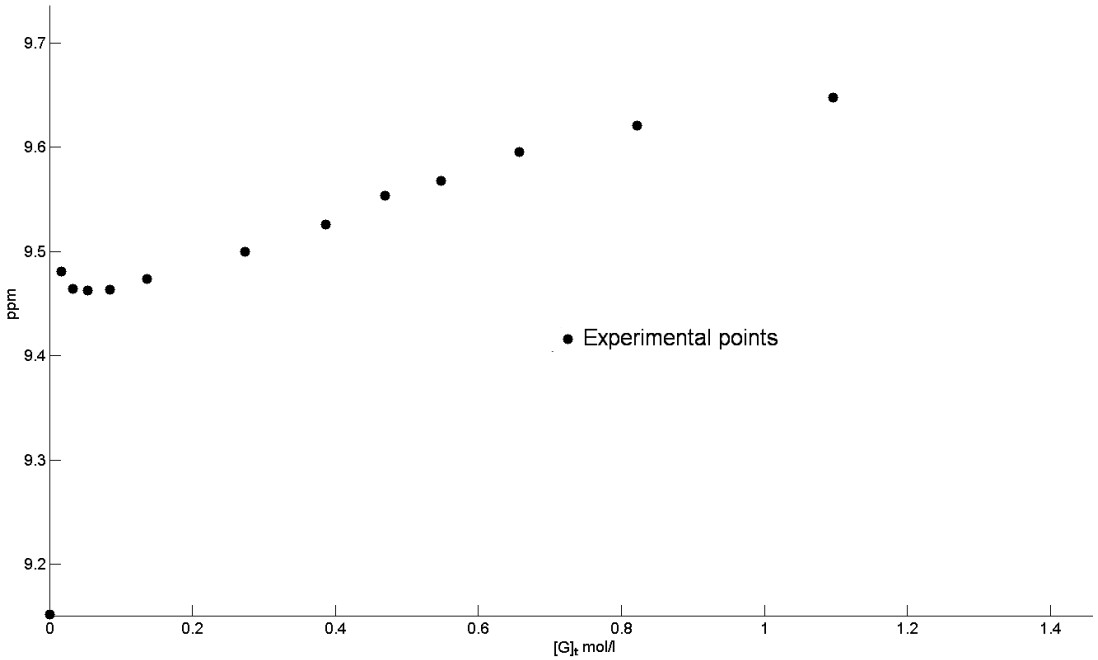

Figure 16: *1:1 fitted binding isotherm of ^{1}H-NMR NH signal of DiBrBzOxP titrated by S-Ibuprofen (0.00068mol/l, $CDCl_3$, 25°C)*

6.2.3 Variable temperature

On figure 17 it is shown that low temperatures cause downfield shift of $\beta-$protons and also decrease the difference in shielding. However because low temperatures slow down exchange rate and equation (106) is not valid anymore. No exact facts can be concluded from this measurement until the rate of exchange is determined.

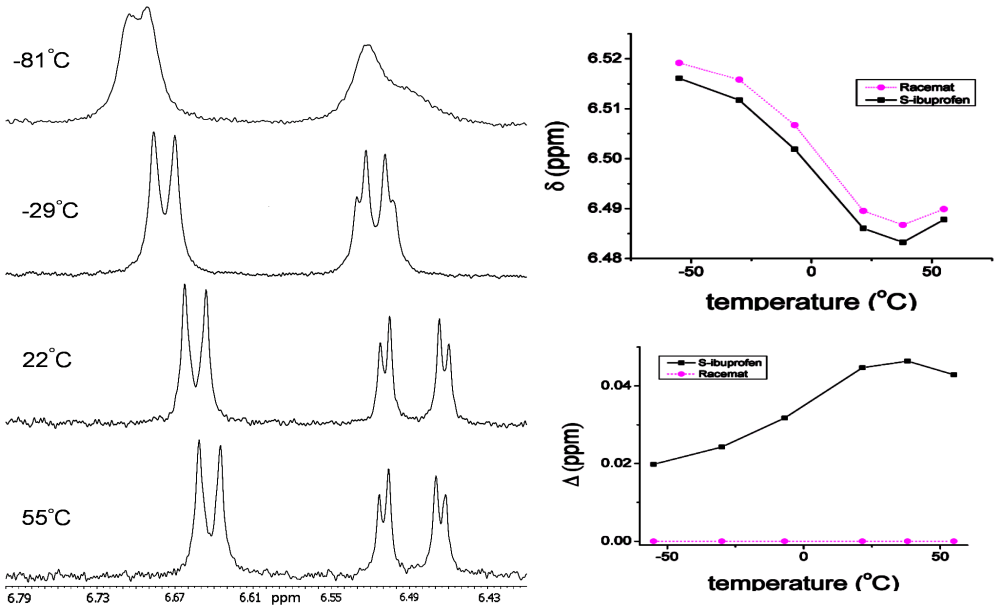

Figure 17: *Variable temperature partial* ^1H *NMR spectra of DiBrBzOxP (0.00068mol/l,* $CDCl_3$*)in the presence of 344 molar equivalents of S-Ibuprofen.*

6.2.4 Optical spectroscopy

The presence of cyclohexadienylidene groups on tetrapyrrole macrocycle have an important influence on its conjugation and conformation. This part of work is concerned with conformational changes induced by their conversion into hydroxyphenyl groups. Protonation of cyclohexadienylidene converts it into a hydroxyphenyl. Because these protonated species undergo conformational changes, guest acidity can influence strength, conformation and dynamics of a complex. To explore effect of protonation on a complex conformation, we decided to study protonation of uncomplexed DiBrBzOxP alone at first. Since these processes are fast on the NMR time scale, we have chosen optical spectroscopy methods.
29 consecutive UV/vis and Raman spectra of $6.10^{-6} mol/l$ DiBrBzOxP solution in deuterochloroform with various amount of trifluoroacetic acid added were measured ($25°C$, 0-8888 molar equivalents). All Raman spectra were normalized to deuterochloroform signal which was then subtracted.

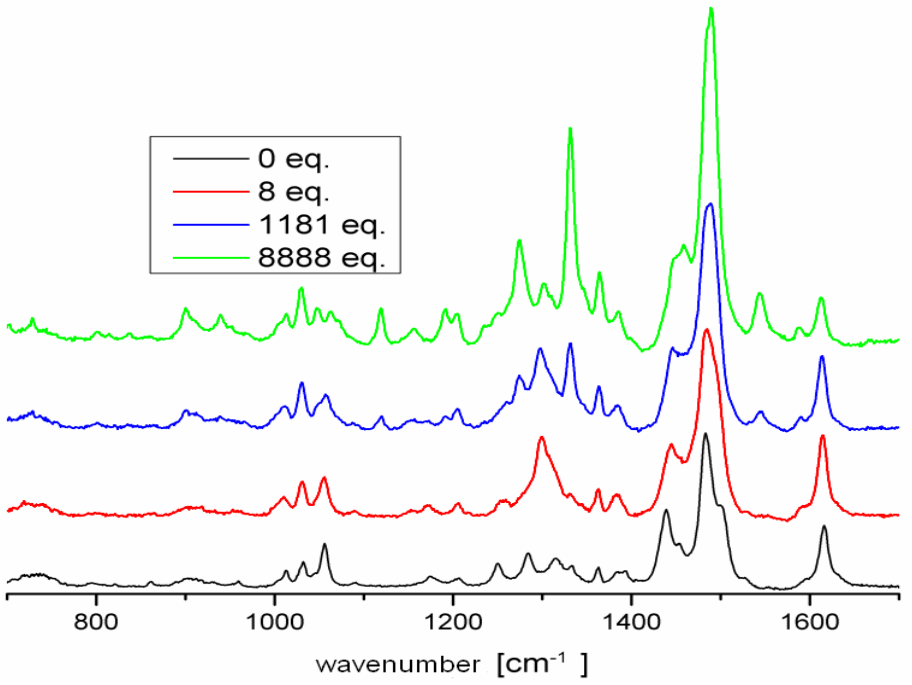

Figure 18: Solvent corrected Raman spectra of $6.10^{-6} mol/l$ *DiBrBzOxP solution* $(CDCl_3, 25°C)$ *with various amounts of trifluoroacetic acid added*

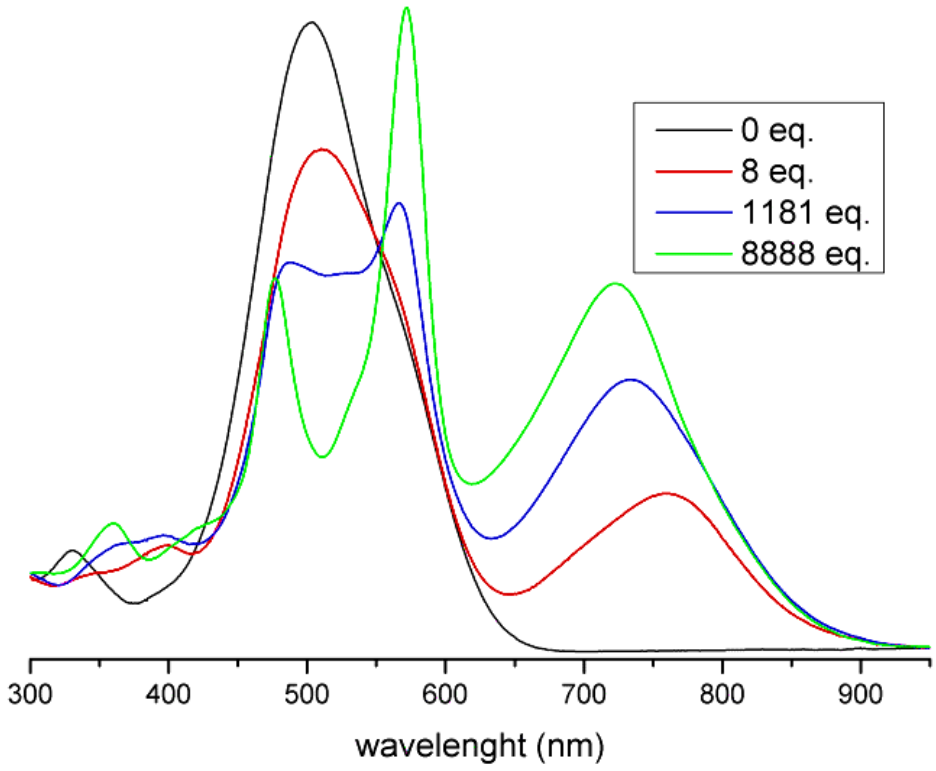

Figure 19: *Absorption UV-vis spectra of* $6.10^{-6} mol/l$ *DiBrBzOxP solution* $(CD_3CL, 25°C)$ *with various amounts of trifluoroacetic acid adde*d

From UV-vis titration can be concluded, that addition of trifluoroacetic acid causes disturbance of electronic structure of DiBrBzOxP. This can be ascribed to protonation of a molecule. UV-vis absorption spectra follow similar trend as OxP followed with addition of mandelic acid (intensification of a new absorption band at 789 nm together with absorption decrease of Soret band, figure 5). But we have used stronger acid, and titrated further to higher molar equivalents. Therefore more protonated forms of DiBrBzOxP might be present in a solution. To confirm this,

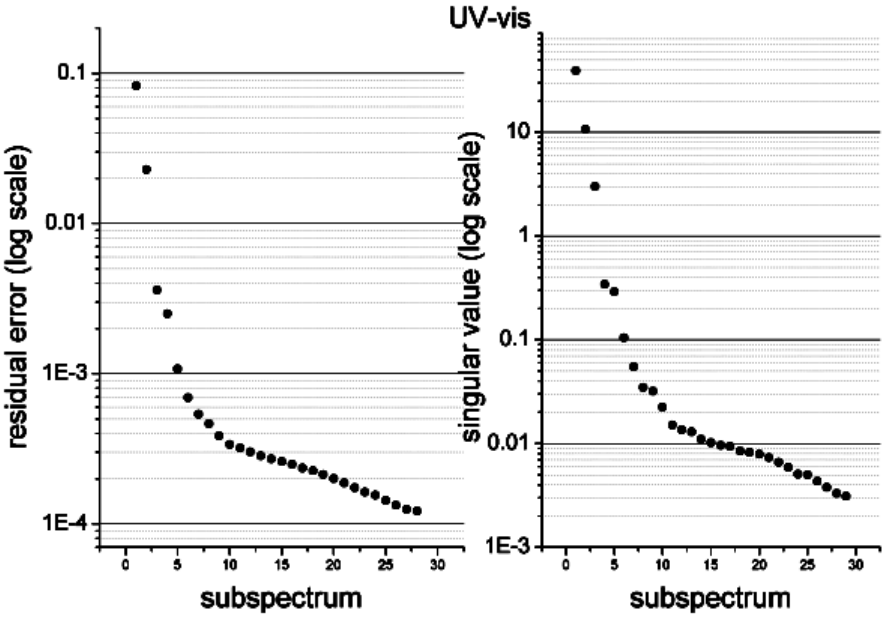

Figure 20: *Singular values (right) and residual errors (left) of each decomposed subspectrum in UV-vis titration.*

quantitative analysis of different forms was performed using SVD.
Each titration spectrum ($Y_i(\nu)$) was decomposed into a set of orthonormal subspectra $S_j(\nu)$ (equation 114). Where W_j are statistical weights (called singular values) of j-th subspectra and the elements V_{ij} present spectral contributions of $S_j(\nu)$ to $Y_i(\nu)$. Each i-th titration spectrum can be therefore expressed as

$$Y_i(\nu) = \sum_j W_j V_{ij} S_j(\nu) \tag{114}$$

SVD for both Raman and UV-vis titrations revealed five significant linearly independent subspectra $S_j(\nu)$ that contribute to original spectra other than noise and baseline deviations (figures 20 and 21).
These 5 subspectra were used to construct pure spectra of the five spectral forms (in our case differently protonated forms of DiBrBzOxP). The idea is based on an assumption that each experimental spectrum can be also expressed as

$$Y_i(\nu) = \sum_{k=1}^{5} c_{ik} Z_k(\nu) \tag{115}$$

c_{ik} is a relative molar concentration of k-th spectral form from i-th measured spectrum, and $Z_k(\nu)$ is a pure spectrum on k-th form. Each $Z_k(\nu)$ can be also expressed as a combination of subspectra $S_j(\nu)$

$$Z_k(\nu) = \sum_{j=1}^{5} R_{kj} S_j(\nu) \tag{116}$$

R_{kj} is a rotation matrix that was determined minimizing the expression

$$\sum_{i,j,k} (c_{ik} R_{kj} - W_j V_{ij})^2 \tag{117}$$

Therefore in principle pure spectral forms $Z_k(\nu)$ and their relative concentrations c_{ik} can be determined.
Because minimizing the equation 117 lead to an infinite number of solutions, two additional constraints were imposed. No negative intensities in spectra of pure forms can be obtained, and

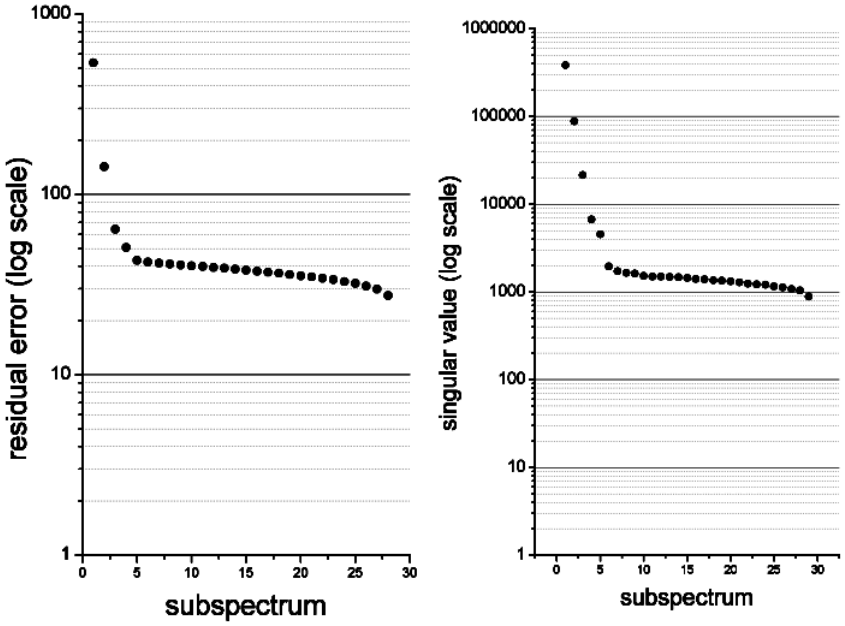

Figure 21: *Singular values (right) and residual errors (left) of each decomposed subspectrum in Raman titration.*

concentration of each individual form should follow acid-base transition:

$$[c]_k = \prod_{j=k}^{j=0} \frac{K_j}{[T]^j} \left(\frac{1}{\sum_{j=0}^{t-1} \frac{\prod_{j=0}^{t-1} K_j}{[T]^j}} \right) \tag{118}$$

$[c]_k$ is a relative concentration of k-protonated form of DiBrBzOxP, $[T]$ is a molar equivalent of trifluoroacetic acid, K_j is an equilibrium constant (expressed in molar fractions) between j-th a (j-1)-th protonated form and t indicates total number of protonated forms.
Using this constraints we were not able to minimize equation 117 for all five forms. From figures 25 and 26 it is clear, that 4-th and higher subspectra $(S_j(\nu), j \geq 4)$ contribute only after 17-th spectrum $(Y_i(\nu), i > 17)$. So we used only first three subspectra $(S_j(\nu), j = 1, 2, 3)$ constructed from restricted range of spectra $(Y_i(\nu), i \leq 17)$, to find three spectral forms $(Z_k(\nu), k = 1, 2, 3)$.

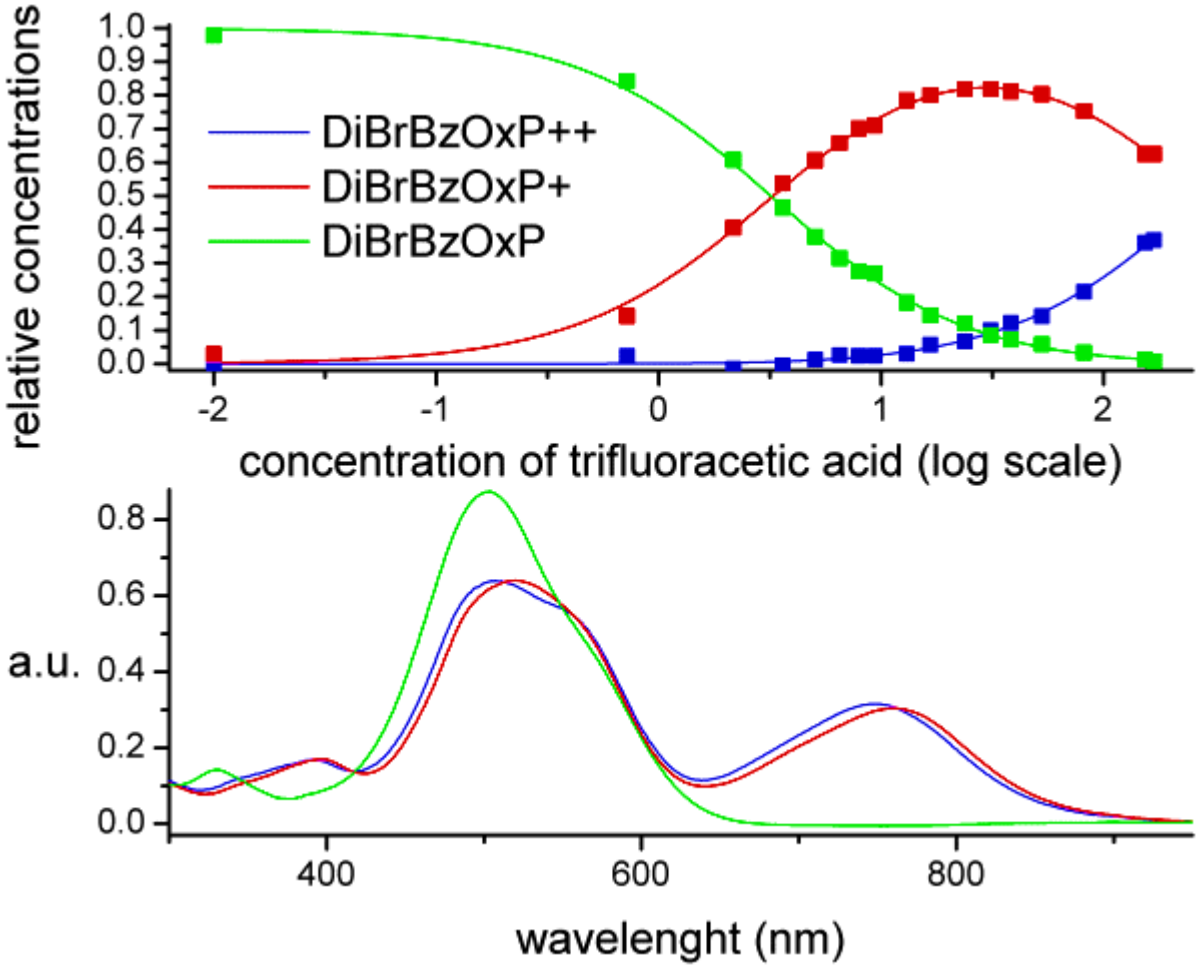

Figure 22: *Relative concentrations (up) and spectra (down) of individual spectral forms from SVD of UV-vis spectra of DiBrBzOxP ($(6.10^{-6} mol/l$, $CDCl_3$, $25°C)$) with different amounts of trifluoroacetic acid added.*

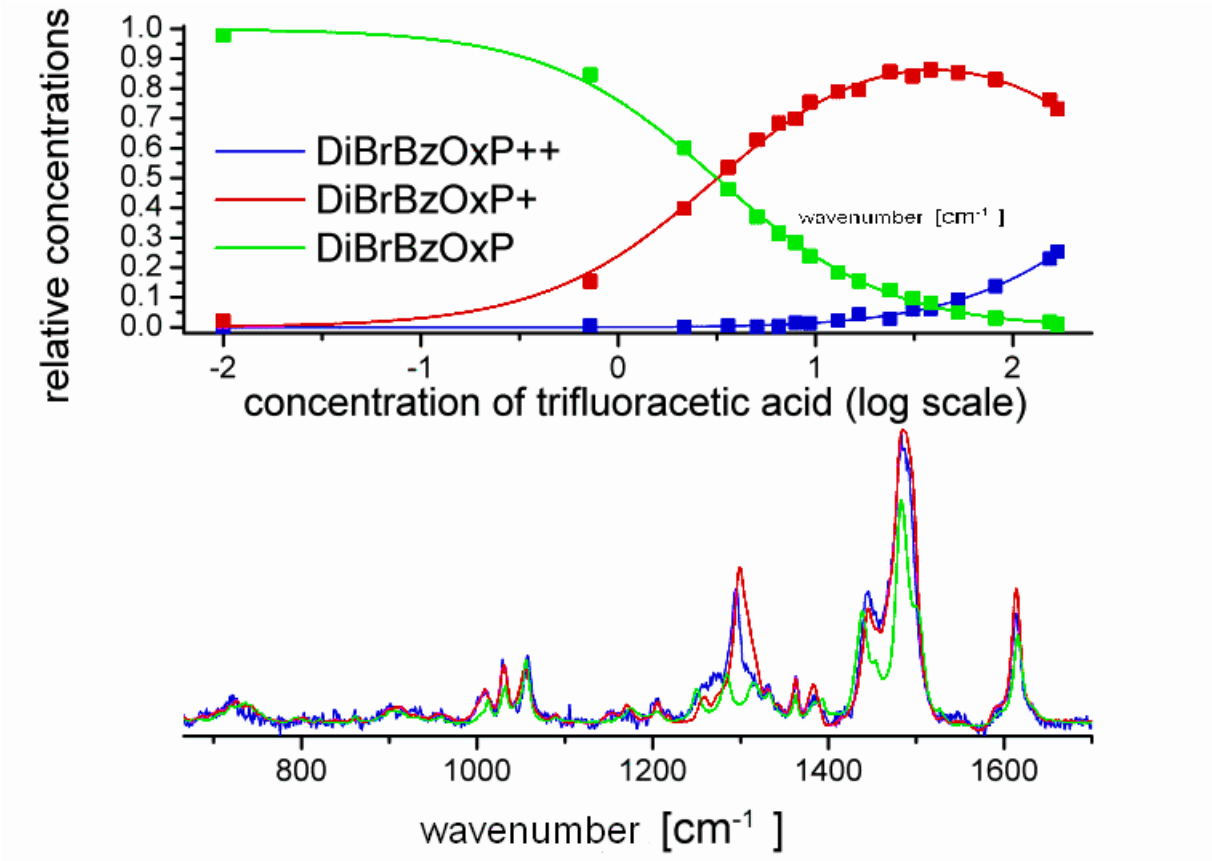

Figure 23: *Relative concentrations (up) and spectra (down) of individual spectral forms from SVD of Raman spectra of DiBrBzOxP ((6.10^{-6}mol/l, $CDCl_3$, 25°C)) with different amounts of trifluoroacetic acid added.*

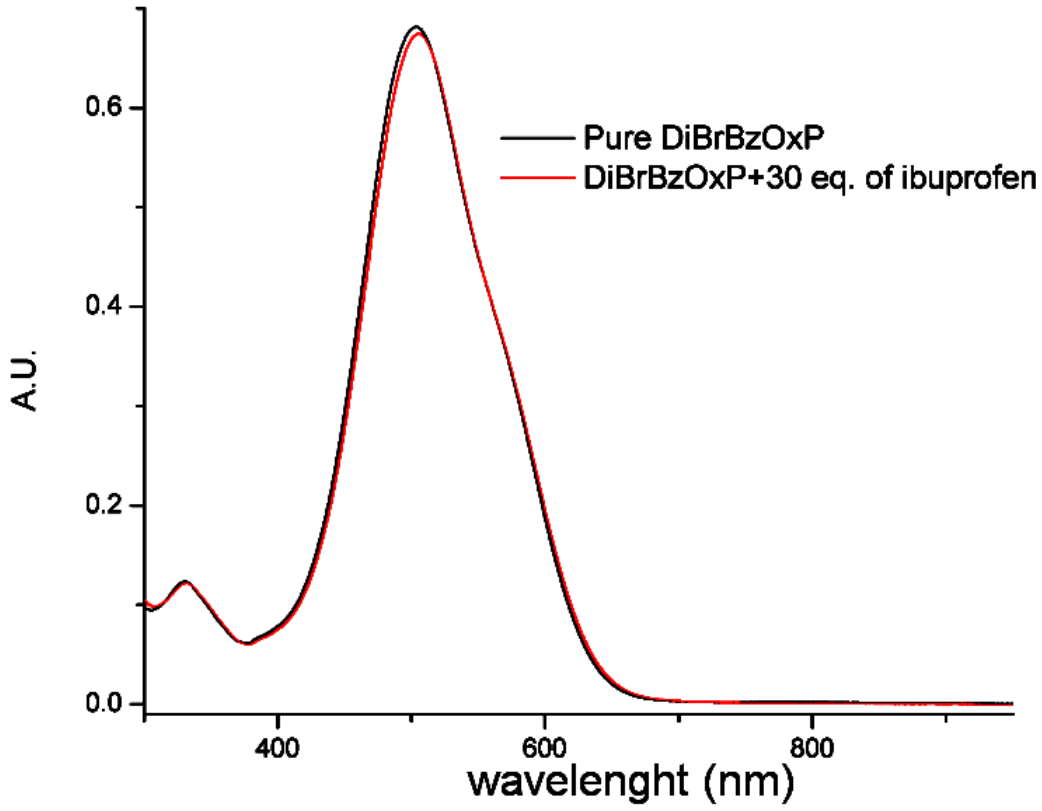

Figure 24: *UV-vis spectrum of DiBrBzOxP ((6.10^{-6}mol/l, $CDCl_3$, 25°C)) with 30 eq. of ibuprofen added.*

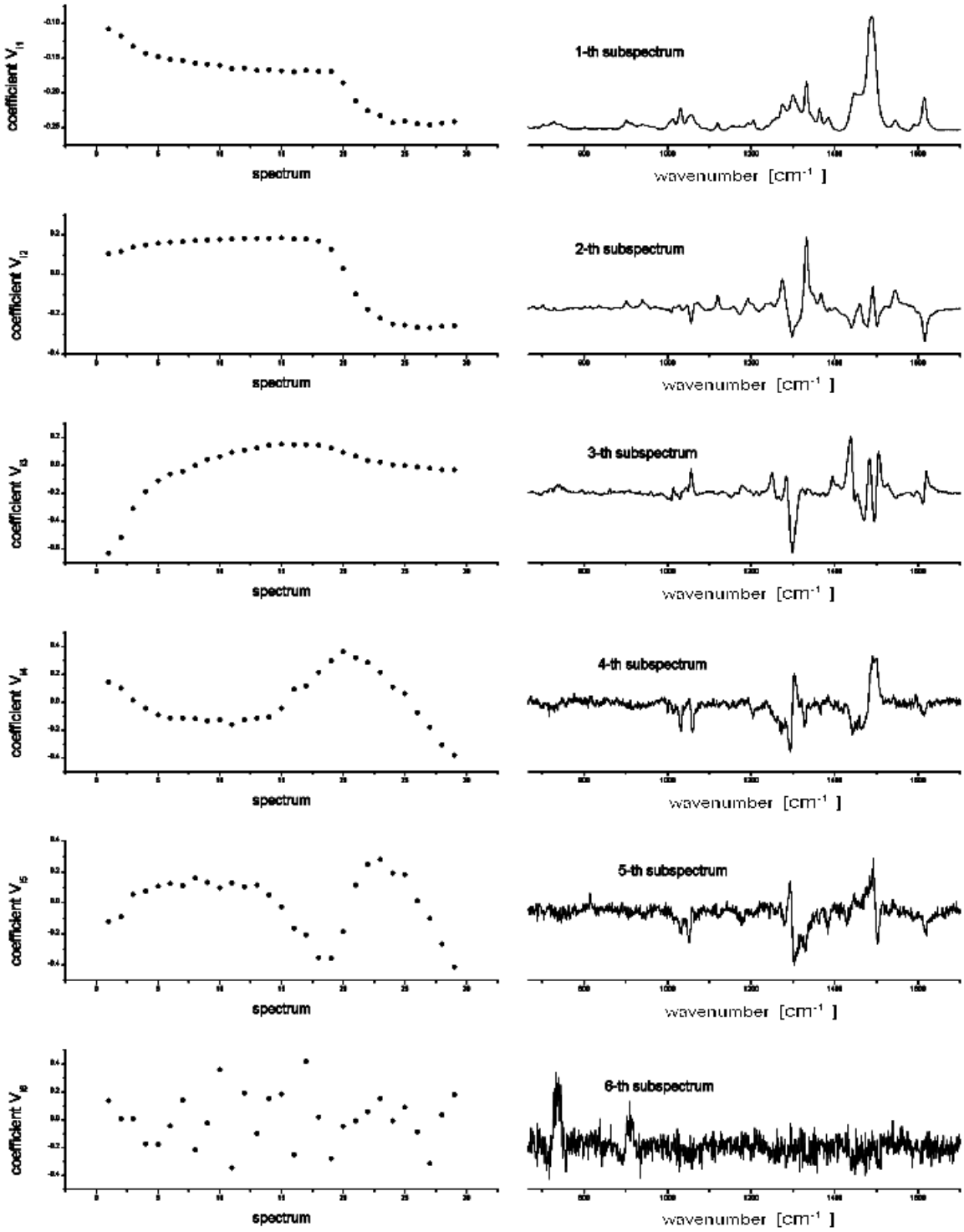

Figure 25: *V_{ij} coefficients with their corresponding subspectral contributions $S_j(\nu)$ from singular value decomposition of the dataset consisting of Raman spectra of DiBrBzOxP ((6.10^{-6}mol/l, $CDCl_3$, 25°C)) with different amounts of trifluoroacetic acid added.*

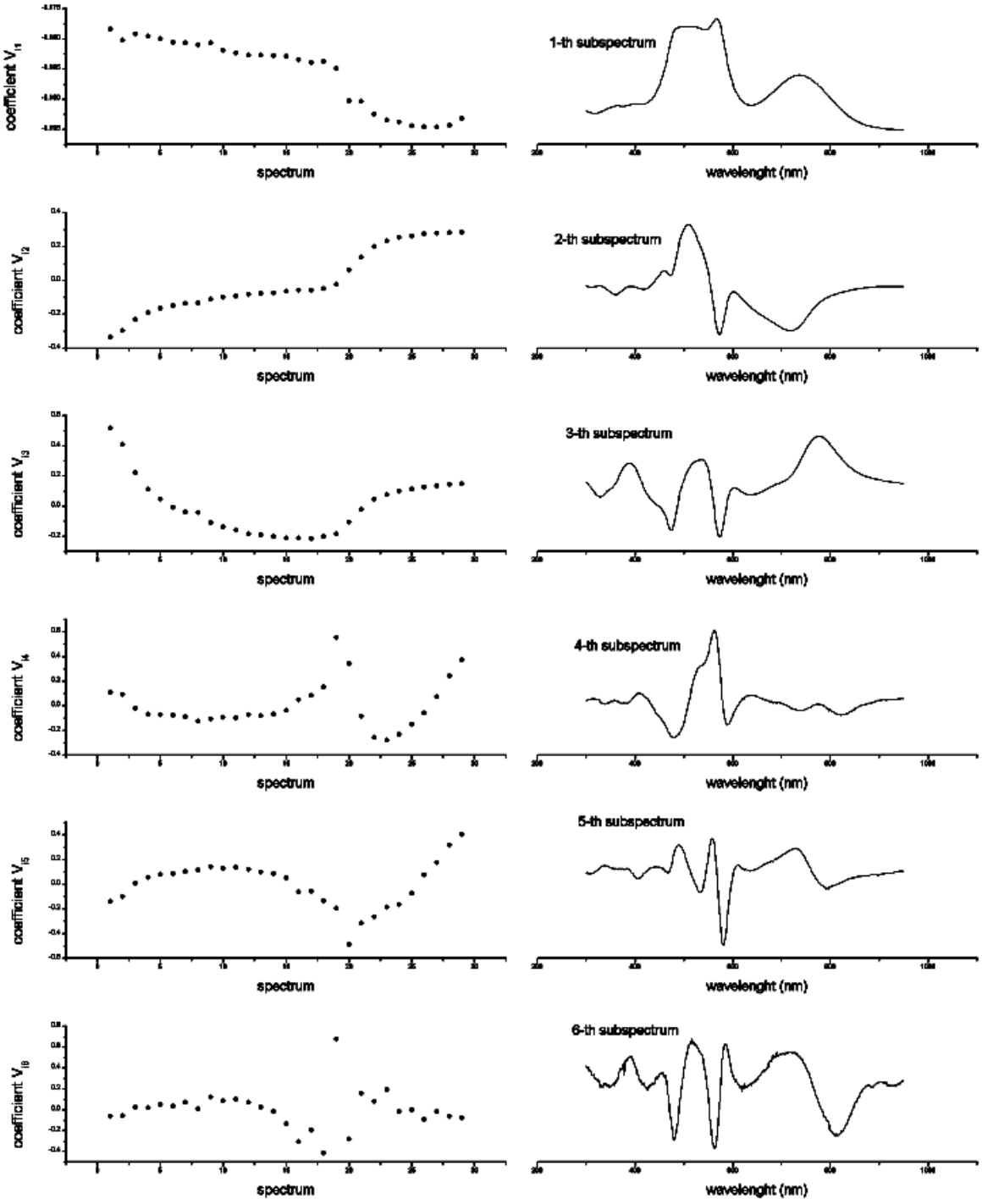

Figure 26: *V_{ij} coefficients with their corresponding subspectral contributions $S_j(\nu)$ from singular value decomposition of the dataset consisting of UV-vis spectra of DiBrBzOxP ($(6.10^{-6} mol/l$, $CDCl_3$, 25°C)) with different amounts of trifluoroacetic acid added.*

We see that decomposition to individual spectral components of UV-vis and Raman spectra both resulted in a very similar concentration curves (figures 22 and 23). equilibrium constants obtained from SVD are $K_1 = 3.23$ and $K_2 = 378$ from UV-vis spectra and $K_1 = 3.17$ and $K_2 = 397$ from Raman spectra. We have demonstrated the existence of two protonated forms of DiBrBzOxP and found their UV-vis and Raman spectra. These protonations take place at carbonyl groups converting oxocyclohexadien groups to hydroxyphenyl groups, thus altering conjugation of tetrapyrrole skelet.

The reason why other two spectral forms did not fit into our model could be caused by two assumptions that we have made. First it was assumed that activity of trifluoroacetic acid remained constant. It is well known fact that at higher concentrations the activity of acid decreases. Another reason is, that those two spectral forms might not be higher protonated forms, but some

non-reversible reaction might be happening. As can be seen from figure 24, no signs of protonation were observed when 30 eq. of Ibuprofen were added into a chloroform solution of DiBrBzOxP.

7 Computations

DiBrBzOxP-Ibuprofen complex contains 884 electrons (602 of which were valence), therefore post Hartree-Fock methods were out of question. Hartree-Fock and it's semiempirical versions (like INDO, AM1, PM3) can not give NMR spectra with desired accuracy. So we decided to model our complex using DFT, which is well known for its excellent performance-to-cost ratio. Because complex is entirely non-covalent, we were careful about a choice of particular functional. Standard and most popular DFT functional B3LYP[40] underestimates bonding energy of hydrogen bonds and overestimates their length[41-43], cannot successfully describe π-hydrogen bonding[44] and also fails completely for dispersion interactions. In 1995, Hobza and coworkers stated that "DFT methods with currently available functionals failed completely for London-type clusters for which no minimum was found"[45]. Since then a new family of functionals, called meta functionals were introduced. This meta functionals include kinetic energy density, which involves second derivatives of occupied Kohn-Sham orbitals. Kinetic energy density term improves their prediction of dispersion forces[46].
For this work we have chosen M-GGA[31] non-hybrid functional M06-L[47], which in many studies performed well for a range of systems, like zeolites [48], magnetic properties [49], water clusters [50] and non-covalent interactions [51]. It also performed best from my own benchmark on GIAO calculated ^{1}H-NMR shifts[32] for oxoporphirinogen molecule. M06-L is computationally less expensive than the meta-hybrid functionals, which allowed us to use polarized basis set for our relatively large system.

7.1 Methods

To fully capture the conformational behavior of DiBrBzOxP+S-Ibuprofen complex, we calculated NMR spectra and Gibbs free energies of formation and compared them with experimental data. All calculations were performed in gas phase using GAUSSIAN 09[52]. Two-electron integrals and their derivatives were calculated using a pruned (99,590) grid[53]. Geometries of the complex were fully optimized using M06-L density functional with Pople's 6-31G(d,p) basis set[54]. To ensure that calculated structures are local minima on a potential energy surface, frequency calculations were performed and no negative vibrational frequencies of nuclei were found.
Gibbs energies were obtained from counterpoise (CP) corrected[55] interaction energies by adding Gibbs corrections obtained from harmonic vibrational analysis as described in section 3.4 of this work. The Gibbs correction is equal to the sum of the Gibbs corrections of the complex obtained from DFT calculations minus the sum of the Gibbs corrections of R-Ibuprofen and DiBrBzOxP obtained at same level of theory. Interaction energy is DFT energy of complex molecule minus energy of DiBrBzOxP and R-Ibuprofen.
Isotropically averaged nuclear magnetic shielding tensors for hydrogen atoms were calculated at the optimized geometries using the GIAO/M06-L/6-31++G(d,p) method. To obtain chemical shift, shielding tensor values were subtracted from shielding tensor values of TMS, that was optimized and calculated at same level of theory. The conversion of calculated shielding tensors into chemical shifts using calculated TMS values improves the results because of systematic error cancellation.
In order to reduce computational cost and to account for scalar relativistic effects, Stuttgart effective core potential (ECP) for core electrons and its corresponding valence basis sets for valence electrons [56] were used for bromine atoms in all calculations. SDD valence basis set was augmented with d functions (exponent 0.389), to account for polarization functions in Pople's basis set.

[31] meta-generalized-gradient-approximation

[32] Benchmark was performed on OxP molecule, which was gas phase optimized with B3LYP/6-31G(d,p). In order to minimize the error from finite basis set and determine the performance of given functional, NMR shielding was calculated with Pople's 6-311++G(2d,2p).

7.2 Results

We have found two stable conformers (figure 27). They were both created by hydrogen bonding of carboxyl group at R-Ibuprofen with two NH groups peeping out of tetrapyrrole macrocycle. Their geometry was adjusted by interaction between benzene ring of R-Ibuprofen and β protons, and possibly $\pi - \pi$ interaction between benzene ring of R-Ibuprofen and quinoid of DiBrBzOxP.

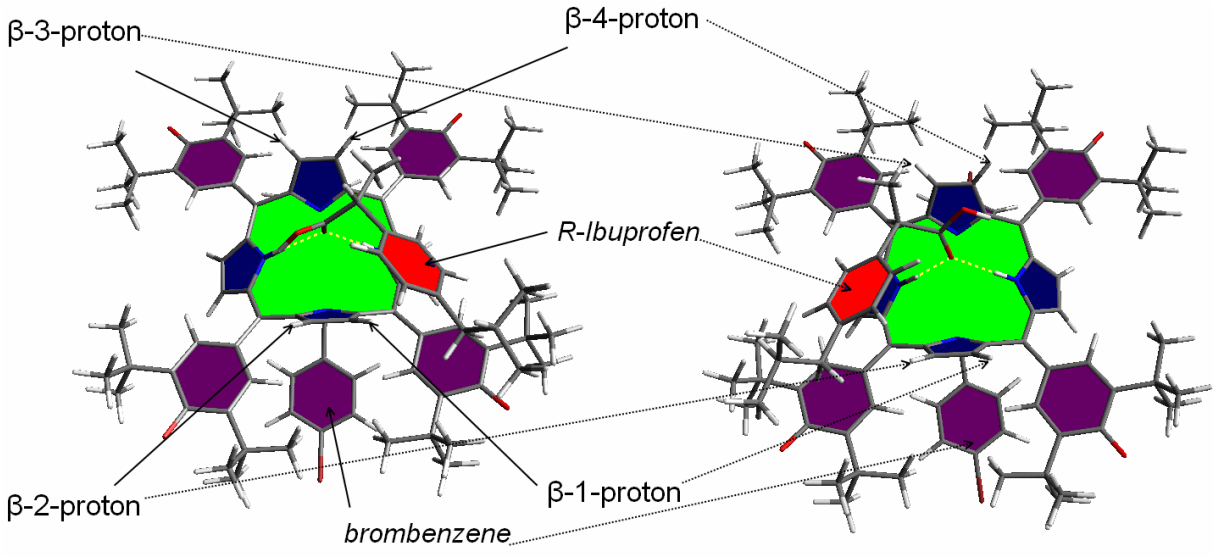

Figure 27: *Two gas phase M06-L/6-31G(d,p) optimized conformers of DiBrBzOxP+R-Ibuprofen complex HG1* **(left)** *and HG2* **(right)**. *Hydrogen bond (yellow dotted line) between Ibuprofen's carboxyl group and DiBrBzOxP NH protons responsible for complex formation is visible.*

Interaction energies with and without Gibbs free energy corrections at 298.15 K and 1 atm. can be found in table 1. Even though gas phase Gibbs free energies may not be directly correlated with experimentally determined Gibbs free energies in solution, the gas phase values found are appropriate for relative comparison of the two conformers.

	interaction energy (kJ/mol)	CP corrected orbital energy (kJ/mol)	$\text{Gibbs}_{298.15K}$ and CP corrected orbital energy (kJ/mol)	conformer population (%)
HG1	-131,34	-107,09	-32,44	10.25
HG2	-131,25	-107,04	-37,81	89.75

Table 1: *Thermodynamic parameters of two stable conformers (figure 27) obtained from M06-L/6-31G(d,p) level of theory*

Relative populations of two conformers (i=1,2) were obtained from Maxwell–Boltzmann distribution using calculated Gibbs energies:

$$[HG_i] \approx \exp\left(\frac{\triangle G_i^{298,15K}}{k_B T}\right)$$

Table 2 shows correlation between the experimental and calculated ^1H chemical shifts for DiBrBzOxP. Mean absolute error for calculated shifts compared with experimental values (figure 8) was 0.25ppm. This satisfactory result for uncomplexed DiBrBzOxP indicates, that chosen level of theory should be sufficient for description of complex. Also note that we are looking for difference in shielding of β-protons in complex, therefore cancellation of errors will further decrease computational error.

	NH	quinon (yellow)	brombenzen (purple)	quinon (dark blue)	pyrrole (green)	brombenzen (brown)	pyrrol (blue)	CH_2 (red)	tert-butyl (black)	tert-butyl (gray)
exp. shift	*7.77*	*7.58*	*7.27*	*6.98*	*6.91*	*6.66*	*6.57*	*4.42*	*1.36*	*1.23*
calc. shift	**7.96**	**7.58**	**7**	**6.82**	**7.21**	**7.56**	**6.84**	**4.5**	**1.54**	**1.38**
abs. error	0.19	0	0.27	0.16	0.3	0.9	0.27	0.08	0.18	0.15

Table 2: *^{1}H-NMR shifts of DiBrBzOxP calculated at GIAO/M06-L/6-31++G(d,p) for gas phase structures (figure 27), compared to experimental data (figure 8). In this figure color legend for individual signals can also be found. All values are in ppm units.*

DiBrBzOxP has C_2 symmetry axis that coincides with oxygen atom involved in hydrogen bond (figure 28). Therefore complex conformation is invariant under 180° rotation of Ibuprofen molecule around this axis. So β-1-proton is twined with β-3-proton and β-2-proton with β-4-proton. This two conformations are equivalent, so they have same energy of formation. Also because of fast exchange between them, it is not possible to detect these conformations. Only an averaged signal from each pair of twinned protons is detected. This explains why β-proton singlet peak (figure 8) splits into two signals, each being a doublet, when complex is formed[33] (figure 9).
In order to relate calculated data with experiment, the chemical shifts values were averaged according to chemical exchanges. Arithmetic average chemical shift values for twined protons were used, and because complex exists in two different conformations, the weighted average of their chemical shift values were used (table 3). Relative population of the two conformers can be found in table 1.

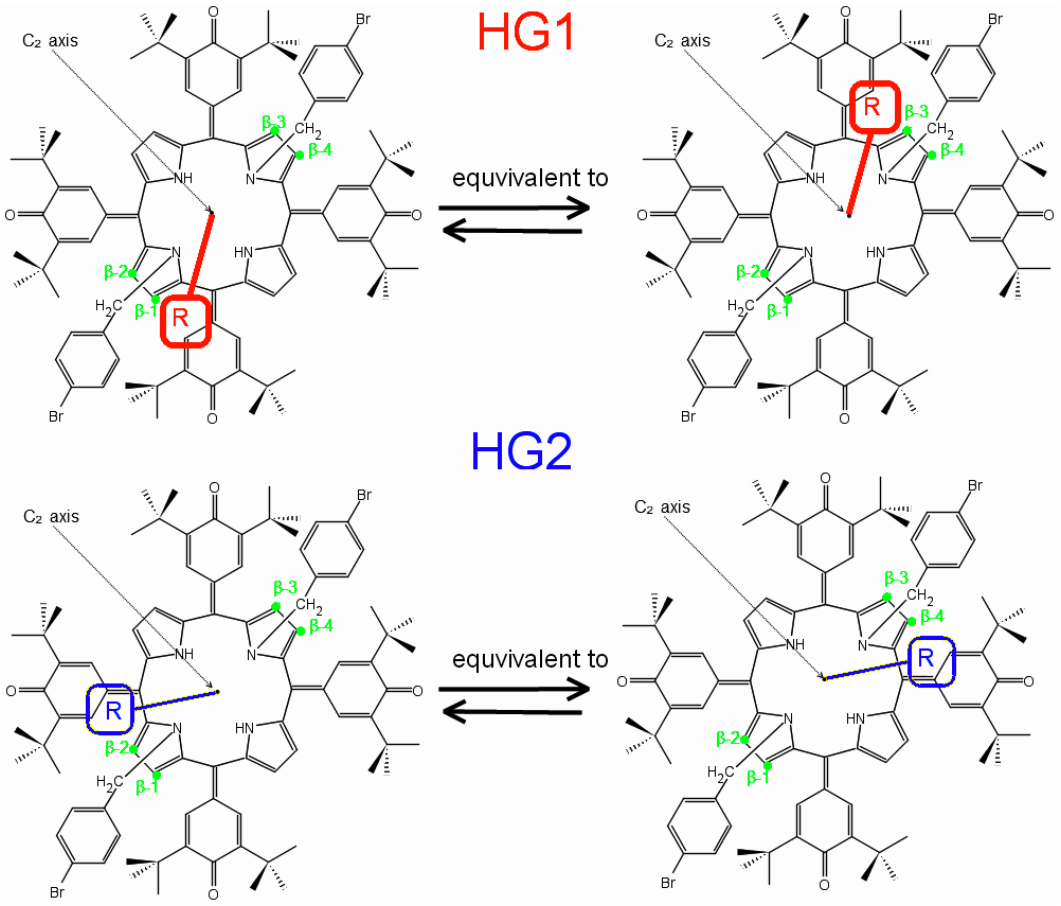

Figure 28: *Schematic illustration of two conformations (and their equivalent versions) for DiBrBzOxP+R-Ibuprofen complex. Chiral R-Ibuprofen induces non-equivalency between adjacent pyrrolic protons, which causes anisochronicity of their resonant frequencies($\Delta \neq 0$).*

[33]The doublet structure arises from J-coupling between adjacent protons.

	DiBrBzOxP	HG1	HG2	weighted HG1 and HG2
β-1 and β-3 proton	6.84	5.68	6.47	6.39
β-2 and β-4 proton	6.84	6.62	6.02	6.08
Δ	0	-0.94	0.45	**0.31**
δ	6.84	6.15	6.24	**6.23**

	Δ	δ
experimental values	*0.28*	*6.15*
computed values	**0.31**	**6.23**

Table 3: *Summary of computed chemical shift values for β-protons obtained from GIAO/M06-L/6-31++G(d,p)* **(up)**. *Comparison with experimental values obtained from extrapolation of titration curves (figure 15)* **(down)**. *All values are in ppm units.*

In table 3 we see that after all averaging is performed, the comparison of calculated NMR parameters agrees well with experimental data. This is a strong evidence that conformations we have obtained correspond to reality. The calculated Gibbs energies of formation are much higher than experimentally obtained values ($-32,44 kJ/mol$ for HG1 and $-37.81 kJ/mol$ for HG2 vs. $-4.44 kJ/mol$ for experimental value). But this is normal, because Gibbs energies measured in liquid solution can not be related to gas phase calculated values.
Binding of S-Ibuprofen shields the adjacent β-protons in opposite direction as R-Ibuprofen does (figure 29). This explains why experimentally determined chemical shift difference Δ exhibit linear dependence on %ee in fast exchange regime (figure 11).

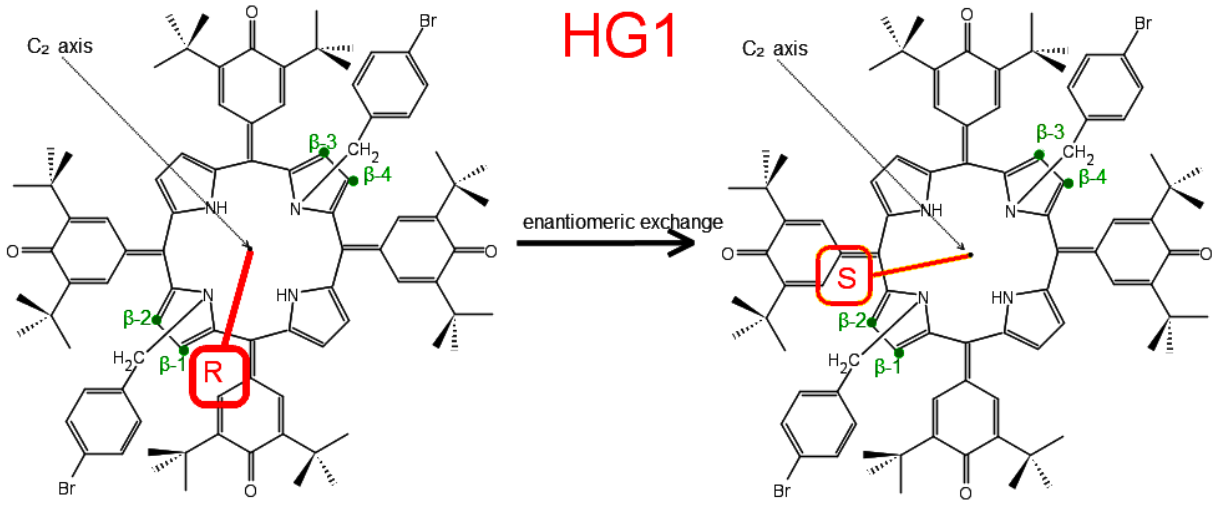

Figure 29: *R/S-Ibuprofen environment induces opposite shielding effects for adjacent protons ($\beta-1$ with $\beta-2$ or $\beta-3$ with $\beta-4$) as schematically shown for given conformation. Because of fast chemical exchange, reducing the %ee causes isochronicity (Δ = 0 ppm for 0 %ee in limiting case) as a result of averaging.*

8 Conclusions and remarks

8.1 NMR

We have demonstrated that achiral DiBrBzOxP can be used as a host for detection of chiral information of Ibuprofen in ^{1}H-NMR spectroscopy. In particular, enantiomeric excess can be determined from β-proton chemical shift difference Δ of DiBrBzOxP. It must be stressed that because host is achiral, the complex itself doesn't provide any information about chirality of Ibuprofen. The R-Ibuprofen and S-Ibuprofen complexes with DiBrBzOxP are equivalent in NMR spectroscopy. It is the dynamics of complex formation and fast exchange of molecules on binding

site, that only provides information about an excess of one enantiomer over the other. Thus only an absolute value, but not the sign of enantiomeric excess can be obtained. Unknown sign can be determined, if one has Ibuprofen of known %ee. Adding a portion of known enantiomeric mixture into unknown sample, and recording the change of %ee that this addition induced, the %ee sign of an unknown sample can be determined.
Chemical shift difference Δ depends not only on %ee, but also on the ratio of complexed to uncomplexed DiBrBzOxP. In order to obtain linear relationship between %ee and Δ, ratio of complexed to uncomplexed DiBrBzOxP must be kept constant. This ratio depends on relative amount of Ibuprofen to DiBrBzOxP in a given solution (figure 10), and because of competitive inhibition caused by water also strongly depends on water concentration in solution (figure 13). This is a problem, because we have shown that even small variation of water concentration (order of $mmol/l$), changes Δ value (figure 13). This high sensitivity to water happens because association constant of water complex is much higher that that of R-Ibuprofen complex ($K_{water} = 255 mol/l^{-1}$, $K_{Ibuprofen} = 6 mol/l^{-1}$). Therefore if one wants to determine %ee of an unknown sample using hypothetical[34] tabulated value of Δ, he has to make sure that not only concentration of Ibuprofen molecule is same as for tabulated value, but also concentration of water must be same. This is especially hard for guest molecules (Ibuprofen also) whose ^{1}H-NMR signals overlap with water signals. In that case, amount of water can not be determined from ^{1}H-NMR signals integration and other analytical method must be used. Alternatively water concentration could be guessed by measuring concentration of water in pure DiBrBzOxP solution, and assuming that water present in guess molecule is either negligible or constant. But we have shown that even for dried Ibuprofen this assumption caused an error, which resulted into a badly fitted binding isotherm and underestimated association constant (figure 15).
Points that are outside fitted curve are those, that have been measured very last during the titration experiment. Water that disturbed the behavior of spectral peaks most probably didn't originated from Ibuprofen, but came from water vapor due to manipulation of sample and its exposure to air. So in order to make this experiment reproducible, it must be performed in water-absent environment.
In variable temperature NMR measurements, we attempted to slow down the chemical exchange to see separate signals from uncomplexed DiBrBzOxP and both complex conformers (figure 17). The lowest temperature that we were able to achieve was not enough to slow down the exchange. It was also observed that decreasing the temperature causes chemical shift difference Δ to decrease and β-1-proton signals were shifted downfield. This can be interpreted, that decreasing the temperature stabilizes the water complex more than Ibuprofen complex. It is only a hypothesis, that can be confirmed or disproved by repeating the temperature varied experiment with samples of different water concentrations. If the observed effect will be stronger for higher water concentrations samples, the hypothesis will be proven.
Alternatively water inhibition can be reduced using a host molecule with higher binding constant to chiral guest. In similar experiment[35], where OxP had been used as a host and mandelic acid as a guest molecule, the binding constant was higher. Because the bonding mechanism between the molecules was same, but the authors detected electronic absorption spectral changes in OxP due to addition of mandelic acid (figure 5). We speculated that increase in binding constant could have been caused by protonation of a host molecule.

8.2 SVD

In order to investigate protonation of DiBrBzOxP molecule, its titration with TFA in chloroform solution was performed, during which successive Raman and UV/vis spectra were recorded. SVD decomposition of Raman and UV/vis spectra revealed five spectral forms during the titration. Three of them have been identified as neutral, single and double protonated DiBrBzOxP (figure 22), and other two remained unidentified. From this analysis, we are now able to determine concentrations of all three protonated forms for given acidity of solution. We intended to study complex of differently protonated forms independently with NMR. But this showed to be impossible, because presence of TFA blocks the binding site of DiBrBzOxP, preventing the complex formation. Therefore to complete this study, an acid that will not block the binding site must

[34] Because there are no tabulated values yet.

be found. Our suggestion is to use carboranes, cage shaped organometallic molecules, known for their high acidity. Carborane acid anion might have much lower affinity to binding site of DiBrBzOxP, which will allow to induce protonation of DiBrBzOxP without blocking the binding site. Also because carboranes are solid at room temperature, they contain less water compared to liquid acids.
From SVD analysis of Raman and UV/vis titration we also obtained pure spectra of protonated forms. Because Raman spectra of these forms differ significantly (figure 18), they are not suitable for determination of abundance of protonated forms. However UV/vis spectra show intensification of new absorption band at 760 nm for protonated DiBrBzOxP, which is moved to 720 nm for doubly protonated DiBrBzOxP (figure 19). This process is accompanied with intensity decrease and splitting of the original absorption band at 505 nm. This distinct changes in UV/vis absorption spectra can be used for straightforward detection of individual protic forms, which determines whether given host causes protonation of DiBrBzOxP molecule. This was immediately performed for Ibuprofen , and we found that Ibuprofen doesn't protonate DiBrBzOxP (figure 24), and we also confirmed that our complex has no ionic bonds.
Interpretation of remaining two forms that appeared when decomposition of all 29 spectra was performed is an open question. We were not able to minimize equation 117 for all 5 forms in a way that will also satisfy equation 118. Equation 118 includes two assumptions:

- It includes only a concentration of TFA, therefore assumes that the activity coefficient of TFA remains constant. This might not be valid for higher concentrations where ionic strength of medium might decrease activity coefficient. To correct this, activity of TFA needs to be used instead of concentration in equation 118.

- It assumes that all forms undergoes reversible acid-base transitions.

If the first assumption is a problem, then replacing concentration of TFA its activity will correctly describe all five spectral forms of DiBrBzOxP. Another interpretation is, that those two forms aren't triple and quadruple protonated forms, but the represent brom-hydrolyzed forms of DiBrBzOxP. Because hydrolysis would be, unlike protonation, an irreversible reaction, it would explain why our model failed. Because those forms appeare only for high concentrations of TFA (more than 1000 molar equivalents), they are not relevant for experiments with single and double protonated forms of DiBrBzOxP.

8.3 DFT

DFT studies revealed two complex conformers (HG1 and HG2). To verify that they agree with reality, we calculated their ^{1}H-NMR chemical shifts and because two conformations undergo fast exchange on NMR scale, calculated shifts were weight-averaged. Where relative populations obtained from calculated Gibbs energies of formation for this conformers were used as weight factors. The Gibbs corrections were too big (74,65kJ/mol for HG1 and 69,23kJ/mol). This is because the molecule has many low frequency modes, some of which may be internal rotations, and so may need to be treated separately. Another problem with low frequency modes is that harmonic approximation might not be valid for them and so ignored anharmonic contributions might be significant.
Because there were deviations even among high frequency modes between those two conformers, we concluded that difference in calculated Gibbs corrections for two conformers might be a real effect. And because for determination of relative populations, only a difference of Gibbs energies is needed, we used those values.
Using calculated relative populations (10.25% for HG1 and 89,75% for HG2) we achieved excellent agreement for chemical shift values (table 3). Because all calculation were performed in gas phase, using moderate basis set and empirical DFT methods, the excellent agreement most probably arouse from fortuitous error cancellation.

8.4 What needs to be done

In summary, we have studied complex from NMR and computational perspective, and protonation from optical spectroscopy perspective. We have found that complex exist in two con-

formations that are not visible in NMR, because they are averaged by fast chemical exchange. NMR spectroscopy revealed that water acts as a inhibitor for complex formation. Optical spectroscopy revealed three different protonated forms, which might have different binding energies with Ibuprofen.

- To minimize inhibition effects of water a more hydrophobic solvent should be used instead of chloroform. The host and guest molecules must be soluble in that solvent, which will be a critical selection rule for solvent.
- Protonation of DiBrBzOxP must be induced with different acid, which won't block its binding site, and protonated complex will be made and studied.
- Solvation model must be included into DFT calculations, for more realistic calculations to be performed.
- Overestimated Gibbs energy correction of DFT calculation must be analyzed, so the relative populations of conformers obtained from those energies will be more credible.
- Variable temperature NMR experiment must be repeated for different water concentrations, so temperature induced spectral changes can be interpreted.
- The interpretation of two unknown spectral forms that appeared during TFA titration needs to be found.

Bibliography

[1]Jerry H. Ginsberg (2008). "§7.2.1 Selection of generalized coordinates". Engineering dynamics, Volume 10 (3rd ed.). Cambridge University Press. p. 397.
[2]Asanov, G. S. Finsler geometry, relativity and gauge theories. Dordrecht, Netherlands : D. Reidel, 1985. p. 370. ISBN 9027719608.
[3]Lam, Kai S. Non-Relativistic Quantum Theory : Dynamics, Symmetry, and Geometry. USA : World Scientific Publishing Company, 2009. 460 s. ISBN 9814271799.
[4]A. Abragam, The Principles of Nuclear Magnetic Resonance, Oxford University Press, Oxford, 1961.
[5]J. Owen, M. Browne, W.D. Knight et al., Phys. Rev. 1956
[6]Levitt, Malcolm H. Spin Dynamics: Basics of Nuclear Magnetic Resonance. England : Wiley, 2001. p. 672 ISBN 0471489220.
[7]Ernst R.R., Bodenhausen G., Wokaun A., Principles of Nuclear Magnetic Resonance in One and Two Dimensions, Clarendon Press, Oxford 1990. ISBN 978-0198556473.
[8]Charles P. Slichter, Principles of Magnetic Resonance, Springer, 1996. p. 672 ISBN 978-3540501572.
[9]Ed Mailly, Eulogy on Quetelet: Abstract of an essay upon his life and works, Smithsonian Institution, 1874.
[10]Cf. I. N. Levine, "Quantum Chemistry," 5th edn, Prentice Hall, Upper Saddle River, New Jersey, 2000, p. 624
[11]P. Hohenberg and W. Kohn, Phys. Rev. B, 1964, 136, 864.
[12]R.G. Parr, W. Yang, Density-Functional Theory of Atoms and Molecules,Section 3.4, Oxford University Press, 1989.
[13]R.G. Parr, W. Yang, Density-Functional Theory of Atoms and Molecules,Section 7.2, Oxford University Press, 1989.
[14]G. N. Merrill, S. Gronert, and S. R. Kass, J. Phys. Chem. A, 1997, 101, 208.
[15]R.E. Moss, Advanced Molecular Quantum Mechanics, Chapman and Hall, London 1973.
[16]Ch.v.Wullen, Chemical Shifts with Hartree–Fock and Density Functional Methods, Calculation of NMR and EPR Parameters, WILEY, 2004, p. 35
[17]J. Gauss, J. F. Stanton, Calculation of NMR and EPR Parameters, Electron-Correlated Methods for the Calculation of NMR Chemical Shifts, WILEY, 2004, p. 125
[18]MCKEE, Michael L. Structures and Mechanisms : From Ashes to Enzymes. Washington D.C. : American Chemical Society, 2002. Application of Theoretical Methods to NMR Chemical Shifts and Coupling Constants, s. 135–149.
[19]W. Bieger, G. Seifert, H. Eschrig et al., Chem. Phys. Lett. 1985, 115, 275.
[20]J. A. Pople, Proc. Roy. Soc. London, Ser. A 1957, 239, p. 541.
[21]M. Schindler, W. Kutzelnigg, J. Chem. Phys. 1982, 76, 1919.
[22]Scatchard, G. Ann. N.Y. Acad. Sci. 1949, 51, 660-672.
[23]Mcquarrie, D. A.; Simon, J. D. Physical Chemistry : A Molecular Approach. USA : University Science Books, 1997. p. 1360.
[24]Horeau, A.; Guette, J. P. Tetrahedron 1974,30, 1923
[25]Rentsch, Katharina M. The importance of stereoselective determination of drugs in the clinical laboratory. Journal of Biochemical and Biophysical Methods. 2002, Volume 54, p. 1-9. ISSN 0165-022X.
[26]Yamaguchi, S. In Asymmetric Synthesis; Morrison, J. D., Ed.; Academic Press: New York, 1983; Vol. 1, Chapter 7, p. 125.
[27]Weisman, G. R. In Asymmetric Synthesis; Morrison, J. D., Ed.; Academic Press: New York, 1983; Vol. 1, Chapter 8
[28]L. R. Milgrom, J. P. Hill, G. Yahioglu, J. Heterocyclic Chem.1995, 32, 97–101.
[29]L. R. Milgrom, Tetrahedron 1983, 39, 3895–3898.
[30]Floriani, C.; Solari, E.; Solari, G.; Chiesi-Villa, A.; Rizzoli, C.Angew. Chem., Int. Ed. Engl. 1998, 37, 2245 2248.
[31]L. R. Milgrom, J. P. Hill, G. Yahioglu, J. Heterocyclic Chem.1995, 32, 97–101.
[32]J. P. Hill, W. Schmitt, A. L. McCarty, K. Ariga, and F. D'Souza, Eur. J. Org. Chem. 2893 (2005).

[33]Jonathan P. Hill, Ian J. Hewitt, Christopher E. Anson, Annie K. Powell, Amy Lea McCarty, Paul A. Karr, Melvin E. Zandler, Francis D'Souza, Highly Nonplanar, Electron Deficient, N-Substituted tetra-Oxocyclohexadienylidene Porphyrinogens: Structural, Computational, and Electrochemical Investigations, The Journal of Organic Chemistry 2004 69 (18), 5861-5869.
[34]Wenzel, T. J.; Wilcox, J. D. Chirality 2003, 15, 256–270.
[35]Atsuomi Shundo, Jan Labuta, Jonathan P. Hill, Shinsuke Ishihara, and Katsuhiko Ariga, Nuclear Magnetic Resonance Signaling of Molecular Chiral Information Using an Achiral Reagent, Journal of the American Chemical Society 2009 131 (27), 9494-9495.
[36]Hanna, M. W.; Ashbaugh, A. L. J. Phys. Chem. 1964, 68, p. 811-816.
[37]Rose, N. J.; Drago, R. S. J. Am. Chem. Soc. 1959, 81, p. 6138-6141.
[38]Amman, P. Meier and A. E. Merbach, J. Magn. Reson. 1982, 46, 319-321.
[39]Dostal, Lubomir. Studium strukturních a fyzikálně-chemických vlastností vybraných acyklických analogů nukleotidů. 2001. p. 76 Diplomova prace. Univerzita Karlova v Praze, MFF, Fyzikální ústav.
[40]Stephens PJ, Devlin FJ, Chabalowski CF, Frisch MJ (1994) J. Phys. Chem. 98:11623
[41]S. Tsuzuki, H.P. Luthi, J. Chem. Phys. 114 (2001) 3949.
[42]J. Sponer, P. Jurecka, P. Hobza, J. Am. Chem. Soc. 126 (2004) 10142.
[43]Tushar van der Wijst, Celia Fonseca Guerra, Marcel Swart, F. Matthias Bickelhaupt, Performance of various density functionals for the hydrogen bonds in DNA base pairs, Chemical Physics Letters, Volume 426, Issues 4-6, 4 August 2006, Pages 415-421, ISSN 0009-2614, DOI: 10.1016/j.cplett.2006.06.057.
[44]How Well Can Density Functional Methods Describe Hydrogen Bonds to π Acceptors?, Yan Zhao„ Oksana Tishchenko, and Donald G. Truhlar, The Journal of Physical Chemistry B 2005 109 (41), 19046-19051
[45]P. Hobza, J. Sponer and T. Reschel, J. Comp. Chem., 1995, 16, 1315.
[46]A. D. Becke, J. Chem. Phys., 1996, 104, 1040.
[47]Y. Zhao, D.G. Truhlar, J. Chem. Phys. 125 (2006) 194101.
[48]Y. Zhao, D.G. Truhlar, J. Phys, Chem. C 112 (2008) 6860.
[49]R. Valero, R. Costa, I.D.P.R. Moreira, D.G. Truhlar, F. Illas, J. Chem. Phys. 128 (2008) 114103.
[50]V.S. Bryantsev, M.S. Diallo, A.C.T. van Duin, W.A. Goddard III, J. Chem. Theor. Comput. 5 (2009) 1016.
[51]D. Benitez, E. Tkatchouk, I.I. Yoon, J. Am. Chem. Soc. 130 (2008) 14928.
[52]Gaussian 09, Revision A.01, M. J. Frisch, G. W. Trucks, H. B. Schlegel, G. E. Scuseria, M. A. Robb, J. R. Cheeseman, G. Scalmani, V. Barone, B. Mennucci, G. A. Petersson, H. Nakatsuji, M. Caricato, X. Li, H. P. Hratchian, A. F. Izmaylov, J. Bloino, G. Zheng, J. L. Sonnenberg, M. Hada, M. Ehara, K. Toyota, R. Fukuda, J. Hasegawa, M. Ishida, T. Nakajima, Y. Honda, O. Kitao, H. Nakai, T. Vreven, J. A. Ontgomery, Jr., J. E. Peralta, F. Ogliaro, M. Bearpark, J. J. Heyd, E. Brothers, K. N. Kudin, V. N. Staroverov, R. Kobayashi, J. Normand, K. Raghavachari, A. Rendell, J. C. Burant, S. S. Iyengar, J. Tomasi, M. Cossi, N. Rega, J. M. Millam, M. Klene, J. E. Knox, J. B. Cross, V. Bakken, C. Adamo, J. Jaramillo, R. Gomperts, R. E. Stratmann, O. Yazyev, A. J. Austin, R. Cammi, C. Pomelli, J. W. Ochterski, R. L. Martin, K. Morokuma, V. G. Zakrzewski, G. A. Voth, P. Salvador, J. J. Dannenberg, S. Dapprich, A. D. Daniels, O. Farkas, J. B. Foresman, J. V. Ortiz, J. Cioslowski, and D. J. Fox, Gaussian, Inc., Wallingford CT, 2009.
[53]V. I. Lebedev and L. Skorokhodov, "Quadrature formulas of orders 41,47 and 53 for the sphere," Russian Acad. Sci. Dokl. Math., 45 (1992) 587-92.
[54]P.C. Hariharan and J.A. Pople, Theoret. Chimica Acta 1973, 28, 213.
[55]S.F. Boys, F. Bernardi, Mol. Phys. 19 (1970) 553.
[56]P. Fuentealba, H. Preuss, H. Stoll, and L. v. Szentpaly, "A Proper Account of Core-polarization with Pseudopotentials - Single Valence-Electron Alkali Compounds," Chem. Phys. Lett., 89 (1982) 418-22.